Micronesica 2015-02: 1–49

Benthic marine diatom flora of Guam: new records, redescription of *Psammodictyon pustulatum* n. comb., n. stat., and three new species (*Colliculoamphora gabgabensis*, *Lauderia excentrica*, and *Rhoiconeis pagoensis*) [1]

CHRISTOPHER S. LOBBAN
Division of Natural Sciences, University of Guam, Mangilao, GU 83823, USA
e-mail: clobban@guam.net

Abstract—Twenty-eight new records and three new species are documented for the Guam flora, extending the records and checklist published in *Micronesica* 43: 237–479. Of note among the new records are *Pinnunavis yarrensis* (Grunow) H. Okuno and *Nitzschia janischii* Grunow both observed alive, plus *Protokeelia cholnokyi* (Giffen) Round & Basson and *Pogoneis bahrainii* Round & Basson seen only in acid-cleaned preparations. *Psammodictyon pustulatum* (Voigt ex Meister) n. comb., n. stat. (Bacillariales: Bacillariaceae) differs from related species in having a pair of rounded elevations on the distal side of the sternum. Three new species are described; only one was observed alive. *Colliculoamphora gabgabensis* (Eunotiales: Eunotiaceae) is smaller and more finely striated than its congeners. *Lauderia excentrica* (Thalassiosirales: Lauderiaceae) differs from the only other species of the genus in having a large, excentric, reniform annulus. *Rhoiconeis pagoensis* (Naviculales: Naviculaceae) differs from the other two known species in its stria density.

Key words: biodiversity, coral reefs, farmer-fish territories, benthic marine diatoms

Abbreviations: DIC: differential interference contrast, LM: light microscopy, RV: raphe valve, SEM: scanning electron microscopy, SV: sternum valve.

Introduction

Although tropical marine benthic diatom floras remain poorly known for the most part (Lobban & Jordan 2010, Riaux-Gobin et al. 2011), our work on the Western Pacific Diatoms Project (Jordan et al. 2009–2015) has made a start on the diatoms of coral reefs in Micronesia, particularly epiphytic species in farmer-fish territories in Guam, with a preliminary checklist for Guam including 237 identified taxa (Lobban et al. 2012). Since then we have added four new species and two new genera: *Licmophora comnavmaria* Lobban & Schefter (2013), *Hanicella moenia* Lobban & Ashworth (2014a), *Lucanicum concatenatum* Lobban & Ashworth (2014b), and *Rhoicosigma parvum* Hein & Lobban (2015). The work of identifying species and sampling habitats in Guam—and even more so in the rest of Micronesia—is still in a very early stage. I present here formal publication of taxa identified since the checklist, which have already been posted on the project website, and descriptions of three species new to science.

---

[1] Citation: Lobban, C.S. 2015. Benthic marine diatom flora of Guam: new records, redescription of *Psammodictyon pustulatum* n. comb., n. stat., and three new species (*Colliculoamphora gabgabensis*, *Lauderia excentrica*, and *Rhoiconeis pagoensis*). *Micronesica* 2015-02, 49 pp. Published online 22 July 2015. http://micronesica.org/volumes/2015
Open access; Creative Commons Attribution-NonCommercial-NoDerivs License.

Methods

Species were identified from continued collection of samples from farmer-fish turfs and other marine habitats on Guam and from continued examination of prior samples. Collection and preparation methods follow previous work and are given in full most recently by Lobban & Ashworth (2014b). Three new sites were sampled, as follows; other sample locations are listed in Lobban et al. (2012, table 1):

GU67 Barracuda Rock commercial dive site, 13.4368 N, 144.6241 E
GU68 Western Shoals, Apra Harbor, 13.4509 N, 144.6556 E
GU69 Abo Cove mangrove, Naval Base Guam, 13.4188 N, 144.6736 E

Results

Records and new species are arranged alphabetically. The taxonomic positions of genera not previously in the checklist are given below; for others see Lobban et al. (2012, table 3). Additional photos of some species are posted on the project website (Jordan et al. 2009–2015).

Amphora rhombica var. *intermedia* Cleve Figs 1–6
Ref. illus.: Peragallo & Peragallo 1897–1908, pl. 50, fig. 3; Wachnicka & Gaiser 2007, fig. 118; Stidolph et al. 2012, pl. 24, fig. 70; Álvarez-Blanco & Blanco 2014, pl. 34, fig. 1.
Samples: GU43C
Dimensions: Length 62–110 μm, width 15–22 μm; dorsal and ventral striae 14–18 in 10 μm
Diagnostics: Radiating striae of transapically elongate areolae; some central interstriae bifurcate toward the dorsal margin; no fascia; central area small; prominent conopeum both internally and externally. Dorsal margin slightly rhomboidal to uniformly curved, the ventral margin nearly straight to slightly arcuate, the raphe branches also nearly straight to slightly arcuate. Apices acute. Numerous copulae with areolae apparently on the pars interior not seen in external SEM view (Fig. 6).
Comments: Differences similar to those shown in the two LM specimens (Figs 1, 2 vs. 3, 4) can be seen in Peragallo & Peragallo's (1897–1908) drawings, one of which is identified as var. *intermedia*; moreover, they noted differences from the original description of the nominate form, but chose not to erect another new variety. Further differences can be seen in size and striae counts of the Guam specimens and the range (for var. *intermedia*) in Wachnicka & Geiser (2007); in particular our small specimens show no differences in stria density from center to apex nor between dorsal and ventral striae. The nominate variety is larger, distinctly semi-rhomboidal, has coarser striae (9–12 in 10 μm), and appears to lack the conopea (Schmidt et al. 1874–1959, pl. 40, fig. 39; Peragallo & Peragallo 1897–1908, Wachnicka & Gaiser 2007). The very fine ventral striation (27 in 10 μm) on the specimen in Witkowski et al. (2000, pl. 168, fig. 12, 13) suggests yet another variety. A species in need of further study.

Common in a diatom coating on reef flat sand, very near low water, where it formed a community with *A. decussata* Grunow and an unidentified *Amphora* sp. among other genera.

Asteromphalus cleveanus Grunow Fig. 7
ASTEROLAMPRALES Round & Crawford: Asterolampraceae H.L. Smith.
Ref. illus.: Hernández-Becerril 1991, pl. 12, fig. 3
Samples: GU52N-4
Dimensions: Length 42 μm, width 33 μm, areolae 16 in 10 μm in the middle of the segment.

Diagnostics: One singular ray reaching the center, 9 ordinary rays around it (i.e., 10 segments), the segments attached to the central area by long costae; small areolae.
Comments: Record based on one broken LM view found in a turf sample from farmer fish territory but presumably redeposited from the plankton. The shape of the valve and the number of rays distinguishes this species from *A. flabellatus* (Brébisson) Greville (Hustedt 1927–1930, fig. 279; Hernández-Becerril 1991, pl. 12, figs 1, 2).

Asteromphalus hepactis (de Brébisson) Ralfs Figs 8, 9
Ref. illus.: Hustedt 1927–1930, fig. 277; Cupp 1943, fig. 32; Hendey 1964, pl. 24, fig. 5; Hernández-Becerril 1991, pl. 28, 29
Samples: GU56A-2, GU52N-4
Dimensions: Length 51 µm, width 47 µm, areolae 5.5 in 10 µm
Diagnostics: One singular ray reaching the center, 6 wide ordinary rays around it (i.e., 7 segments), large areolae.
Comments: Record based on one internal SEM view; the high mantle, shown in Hernández-Becerril's (1991) images is not evident in the vertical image, but the specimen is otherwise consistent with those images and Hustedt's (1927–1930) drawing and description.

Auricula flabelliformis Voigt Figs 10–12
Syn.: *A. machutchoniae* Giffen (1970b)
Ref. illus.: Voigt 1960, pl. 1, figs 8, 9; Ricard 1977, pl. 8, fig. 2; Ricard 1987, fig. 942
Samples: *Guam*: GU66A-2; *Yap*: Y26B
Dimensions: Length 92–95 µm, width 64–67 µm, striae *ca*. 19 in 10 µm; fibulae ca. 8 in 10 µm.
Diagnostics: Large, broadly reniform valve, dorsal margin (defined by the raphe-keel) forming >90% of the circumference, indented from the valve margin before the ventral ends; ventral margin very short, straight. Striation flabellate, arising along a poorly defined median line.
Comments: Observed so far as only a single SEM specimen from Guam and an LM specimen from Yap. Voigt named three varieties besides the type in which the pattern of striae along the median axis ranged from flabelliform to distichous (var. *hustedtii*), the latter based on Meister's (1932, pl. 10, fig. 67) *Hustedtia mirabilis*, now *Auricula mirabilis* (Meister) Paddock & Sims (1980).

Campylodiscus fastuosus Ehrenberg Figs 13, 14, 16, 18–20
Syn: *Campylodiscus thuretii* Brébisson
C. simulans Gregory
Ref. illus: Peragallo & Peragallo 1897–1908, pl. 57, figs 4–9 (as *C. thuretii*); Choi & Noh 1987, figs 73–76; Guettinger 1989 2.09.01-1; López Fuerte et al. 2010, pl. 39, figs 10, 11 (as *C. simulans*); Stidolph et al. 2012, pl. 21, fig. 14 and pl. 6, fig. 132 (the latter as *C. thuretii*)
Samples: **GU66F-7A, GU66F-8, GU52Q-10a, GU52Q-2, GY44Y-13**
Dimensions: 16–34 µm diam., central striae 14 in 10 µm
Diagnostics: Circular valves with two parallel lines of short striae along the apical axis. Small valves similar to *Surirella scalaris* Giffen (Figs 15, 17) (Lobban et al. 2012, pl. 68, figs 5, 6; pl. 69, figs 1, 2), but differing in the marked narrowing of the infundibula such that the spaces between them become wider and with a single prominent rib reaching the central area, whereas in *S. scalaris* the infundibula taper only a little and leave a uniform space between them, without a prominent rib. Both have several spiny ridges over the infundibula on both sides of the raphe; those of *C. fastuosus* are less spiny in comparison.
Comments: The difference is hard to see in small specimens in LM, and we needed complete frustules (Figs 16, 18) before being sure about *C. fastuosus*, which commonly co-occurred with *S. scalaris* in these Guam samples from farmer-fish territories. The LM image published in Lobban et

al. 2012, pl. 68, fig. 4 as *Surirella scalaris* is in fact *C. fastuosus* and a true image is shown here in Fig. 15 for comparison. This has been corrected on the web page. See VanLandingham (1968) for synonymies.

Cocconeis dapalistriata Riaux-Gobin, Romero, Compère & Al-Handel Fig. 21
Ref. illus.: Riaux Gobin et al., 2011, pl. 3, figs 6–8, pls 39, 40.
Samples: **GU44AU-2**
Dimensions: Length ca. 17 μm, width 10 μm, striae ca 10 in 10 μm
Diagnostics: Distinctive striae pattern; the epithet *dapalis*, sumptuous, refers to the "remarkable and magnificent SV striation" (Riaux-Gobin et al. 2011, p. 25).
Comments: Included so far on the basis of a single sternum valve in SEM.

Cocconeis ornata W. Gregory Figs 22–26
Ref. illus.: Gregory 1857, pl. IX (1), fig. 24; Peragallo & Peragallo 1897–1908, pl. 4, figs 13–15; Montgomery 1978, pl. 61, figs A–D; Riaux-Gobin et al. 2014, figs 9–14
Samples: **GU44AU-2**
Dimensions: Length 19 μm, width 15 μm, striae ca 10 in 10 μm
Diagnostics: SV: striae coarsely uniseriate but sometimes branching towards the margin, striae interrupted by a longitudinal hyaline line; margin with parallel rows of papillae. RV not seen.
Comments: A few specimens in this sample. Gregory (1857) was charmed by the "rich ornate aspect" of this "beautiful" species, which does indeed appear ornate, especially in SEM (Fig. 27). The original drawing did not do it justice.

Cocconeis subtilissima Meister Figs 27–32
Ref. illus.: De Stefano & Romero 2005, pl. 32, figs 1–9, pl. 33, figs 1–11; Suzuki et al. 2008, figs. 1–41; Riaux-Gobin et al. 2011, pl. 6, figs 3–11, pl. 73, 74
Samples: **GU44I-2, GU44Z-15, GU44AC-4, GU44AQ-1, GU52P-8**
Dimensions: Length 16–22 μm, width 11–15 μm, striae (SV) 30 in 10 μm, (RV) 32 in 10 μm
Diagnostics: RV (Figs 29, 30) with sigmoid raphe branches, a small hyaline area beyond the terminal raphe endings; central area small, asymmetrical; internal central raphe endings deflect past each other and come to a point. SV alveolate (Figs 31, 32) with slit-like striae divided by a single longitudinal hyaline line; internally a single row of areolae opens from the inner line of alveoli and the other alveolae open via a ring of areolae around the margin.
Comments: De Stefano & Romero (2005) placed this species and others with such alveolate walls (e.g., *C. convexa* Giffen and *C. heteroidea* Meister in our flora) in a new section *Alveolatae*. They also provided tables comparing the alveolate taxa. De Stefano & Romero (2005) distinguish *C. subtilissima* from several species, especially *C. pseudomarginata* Gregory, by the denser striae. The RV of *C. subtilissima* is similar to that of *C. krammeri* (see especially Witkowski et al. 2000, pl. 33, figs 1–4, pl. 42, fig. 34), but the stria density is slightly lower, 23–28 striae in 10 μm; on SV of *C. krammeri* there are 2 longitudinal hyaline lines creating three sets of areolae on each side of the sternum.

***Colliculoamphora gabgabensis* Lobban, n. sp.** Figs 33–40
EUNOTIALES Silva: Eunotiaceae Kützing
Samples: GU44K-6; **GU44I-1, GU44Z-15, GU44W-10, GU44U-1B, GU44AK-6, GU66F-4,** GU66F-8
Dimensions: Length 6.4–11 μm, width 2.8–4.2 μm, striae 25–27 in 10 μm in the middle, denser around the apices.

Diagnosis: Differing from other *Colliculoamphora* species in the smaller size, finer striae, and markedly concave dorsal margin; dorsal striae interrupted by longitudinal hyaline area.
Holotype: GU44AK-6, slide 958, Fig. 33. Deposited at California Academy of Sciences (CAS), accession # 627425, slide # 223041.
Paratypes: A specimen (Fig. 35) is marked on GU44I-1, slide 494, CAS accession # 627427, slide # 220343, in addition to the holotype of *Lauderia excentrica,* and the specimen in Fig. 29 from GU44Z-15 is on a stub deposited at CAS, accession # 627385.
Type locality: GabGab reef, Apra Harbor Guam, 13°26′ 33.63″ N 144° 38′ 34.25″ E, associated with filamentous algal turf in a farmer-fish territory, collected by C. Lobban & M. Schefter, 5 Nov. 2011.
Etymology: named for the type location, which in turn is a Chamorro name for the coral tree (*Erythrina variegata* L.).
Description: Valves linear, asymmetrical about the apical plane, dorsal margin curved, more or less strongly concave, ventral margin slightly bent. Raphe visible on the valve face at each pole but lying mostly on the mantle (Figs 36, 37). Striae on the dorsal side interrupted by an irregular, apparently depressed hyaline area (Figs 36, 37); striae parallel on the proximal side of this area, but on the distal side parallel only in the middle, becoming radiate around the poles, where they also become denser from the interpolation of additional short striae along the margin (Figs 37, 38). Single row of more closely-spaced pores on the ventral side of the raphe (Fig. 38). Copulae areolate (Fig. 40). Valve surface smooth, not colliculated (i.e., lacking small elevations).
Comments: Present in low numbers in several samples and probably overlooked in others. *Colliculoamphora* was established by Williams & Reid (2006) for two species formerly placed in *Amphora*. They noted the similarity to *Eunotia*, from the way the raphe hooks off the valve face onto the mantle, and placed it in Eunotiaceae. Williams & Reid (2009) gave a comprehensive list of the ten known species of *Colliculoamphora*, noted the paucity of material for all species, and rationalized the description of new species on such data as they had, an argument I applaud. Most species have straight or convex dorsal margins but three have concave dorsal margins. Of the latter, *C. palawanensis* G. Reid & D.M. Williams (Williams & Reid 2009, figs 15, 17–21) most closely resembles our species, in having a central hyaline area the length of the valve and the closest shape, but it is larger (14–17 x 4–5 µm) and the striae coarser (18–19 in 10 µm). Indeed, our species is smaller and the striae denser than any in Williams & Reid's (2009) list. No external SEM was given for *C. palawanensis*.

Hemidiscus cuneiformis var. *ventricosa* (Castracane) Hustedt Figs 41, 42
COSCINODISCALES Round & Crawford: Hemidiscaceae Hendey
Ref. illus.: Hustedt 1927–1930, fig. 542d; Hendey 1964, pl. 22, fig. 9; Ricard 1987, figs 30–34; Stidolph et al. 2012, pl. 13, fig. 71 and pl. 4, figs 104, 107; Álvarez-Blanco & Blanco 2014, pl. 11, fig. 6; the images in Round et al. 1990, pp. 192–193, are also evidently this species.
Samples: **GU66F-4**
Dimensions: long axis 71–74 µm, short axis 41–45 µm
Diagnostics: Distinctively shaped, lens-shaped in valve view but the frustules wedge-shaped (cuneiform) because the valve faces are at an angle to one another. Areola pattern similar to *Actinocyclus,* to which it is related, but with a series of radiating patterns around the margin, especially on the less strongly curved side. Large rimoportulae visible in the oblique view (Fig. 42). A pseudonodulus is present on the flatter side (Fig. 41).
Comments: Two valves observed in one sample. The ventral curvatures of *H. cuneiformis* Wallich vary from straight to sinuous and Hustedt combined several older *Eudotia* species as varieties. Images shown by Hendey (1964), Stidolph et al. (2012, pl. 13, fig. 71) and identified simply as *H. cuneiformis* Wallich, have a ventral outline as shown here; Hendey did not comment on varieties; Stidolph et al. (2012, pl. 10, fig. 30) show the nominate variety, again without noting the variety.

The species differs further in valve shape from two fossil species (Harwood & Maruyama 1992). Although Round et al. (1990) (reprinted in AlgaeBase) said that the *valves* are cuneiform, it seems to me that Wallich's (1860) epithet refers to the shape of the *frustule* (described by Round et al. 1990 as "shaped like orange segments"), rather than to the shape of the valve.

***Lauderia excentrica* Lobban, n. sp.** Figs 43–48

THALASSIOSIRALES Glezer & Makarova: Lauderiaceae (Schütt) Lemmermann, emend. F.E. Round & R.M. Crawford

Samples: **GU44I-1**, **GU44Y-13,** GU55B-4, **GU66A-3**

Dimensions: Diameter 23–26 µm.

Diagnosis: Differing from *L. annulata* in the larger, reniform, excentric annulus, in the more numerous fultoportulae over the valve face and mantle, and in lacking a ring of longer spines.

Holotype: GU44I-1, slide 494, deposited at California Academy of Sciences, accession # 627427, slide # 220343. Fig. 43.

Type location: GabGab reef, Apra Harbor Guam, 13°26′ 33.63″ N 144° 38′ 34.25″ E, associated with filamentous algal turf in a farmer-fish territory, collected by C. Lobban & M. Schefter, 29 Oct. 2007.

Etymology: with reference to the excentric annulus.

Description: An asymmetrically placed reniform central area is defined by a hyaline ring from which radiate numerous hyaline veins ("costae"); on the wider side some of these branch dichotomously (Figs 43, 44). Punctae scattered in the central area and usually biseriate between the veins (Figs 44, 45). Fultoportulae scattered in the central area and occurring along the veins over much of the valve face although less frequent in a zone around the central area (Figs 44, 45). Spines absent. Numerous fultoportulae on the margin, where anastomosing costae form a "loculate" pattern, as in *L. annulata* (Figs 44, 47). One large rimoportula at the edge of the valve furthest from the central area, with a simple circular opening externally (Fig. 44) and a large labiate process internally (Figs 46, 48). Fultoportulae in the outer zone are mostly on the veins, whereas those in the zone around the central area are mostly between veins. Fultoportulae consist of a slightly flared external tube 0.5 µm high and a much shorter internal tube (visible on the mantle in Fig. 48); fultoportulae within the annulus generally had no 5 satellite pores, those in the striae had 2–4 (Fig. 48). Valves do not appear to be delicate.

Comments: All previously reported taxa were synonymized by Hasle (1974) into *L. annulata* Cleve, and Round et al. (1990) placed it in its own family. It forms delicate chains in the plankton (Ricard 1987, figs 140, 147). The ultrastructure of the valve was shown by Hasle (1974, figs 1–3, 6–12), Syvertsen & Hasle (1982), Round et al. (1990, pp. 150–151) Güttinger (1994), and Al-Kandari et al. (2009, pl. 5A, B). Hasle (1974) gives the range of valve diameters as 24–75 µm; the new species is at the lowest end of this range. The present species has not been seen alive, and is represented so far only by a few valves from sites both inside the harbor and on the outer coast. It was perhaps deposited from the water column but the valves seem relatively sturdy, unlike *L. annulata*, and it may be benthic [cf. *Roundia cardiophora* (Round) Makarova in our flora]. This species is significant in adding a second taxon to this family.

Mastogloia affirmata (Leuduger-Fortmorel) Cleve Figs 49, 50

Section: Undulatae

Ref. illus.: Hustedt 1931–1959, fig. 962.

Samples: **GU44AX-1**

Dimensions: Length 39 µm; width 22 µm; transapical striae 14 in 10 µm, longitudinal striae 10 in 10 µm except for the wider row adjacent to axial area; partecta 3.3 µm wide, 13 in 10 µm.

Diagnostics: Coarsely areolate, those along the raphe notably elongated; apices produced; longitudinal ribs almost straight; partectae very narrowly rectangular.
Comments: Distinguished from the very similar *M. bahamensis* Cleve (Hustedt 1931–1957, fig 963, Hein et al. 2008, pl. 34, fig. 6 and pl. 36, fig. 10), which has irregularly wavy longitudinal ribs, according to Hustedt, and from *M. subaffirmata* Hustedt (see below) by the much coarser striae. Record based on a single specimen from Guam, but also seen in samples from Yap (unpublished).

Mastogloia emarginata Hustedt Figs 51–55
Section: Ellipticae
Ref. illus.: Hustedt 1931–1959, fig. 896; Pennesi et al. 2013, figs 65, 66 (lectotype specimen)
Samples: **GU44R-2, GU44AU-1; GU53E-2; GU66F-4**; GU55B-4
Dimensions: Length 18–20 µm; width 9–13 µm; striae 20–23 in 10 µm; partecta 2 in 10 µm.
Diagnostics: Small oval valves with 3–4 concave partecta on each side, reaching the apex, pore on the outer side of each partectum distinctively visible in LM (Fig. 54, arrows). Longitudinal striae nearly straight, coarser than the transapical striae, resulting in rectangular areolae.
Comments: Differs from *M. ovulum* Hustedt, which has finer, circular areolae, and partectal pores that are not evident in LM. As noted in the errata to Lobban et al. (2012), the specimen given there in pl. 33, figs 9, 10 for *M. ovulum* was misidentified and is given here correctly as *M. emarginata*; the specimen of *M. ovulum* posted on the web in its place is printed here as Figs 56, 57; see Jordan et al. 2009–2015, /taxa_id/585541, for SEM images of *M. ovulum*. Besides the unique pores, *M. emarginata* differs from *M. ovalis* A. Schmidt in having partecta reaching the apex and from *M. matthaei* (see below) and *M. stellae* (Pennesi et al. 2013, figs 45–52, 57–60) in the number of partecta as well as characters of the areolae.

Mastogloia matthaei Pennesi & Poulin Figs 58–61
Section: Ellipticae
Ref. illus.: Pennesi et al. 2013, figs 37–44, 53–56
Samples: **GU52P-2**
Dimensions: Length 14–15 µm; width 9 µm; striae 24–27 in 10 µm.
Diagnostics: Small oval valves with 3 concave/bilobed partecta on each side, reaching the apex. Quadrangular areolae in irregular longitudinal striae; internal areolae in longitudinal rows (not seen yet in Guam specimens).
Comments: Very similar to *M. ovulum* Hustedt, *M. emarginata* Hustedt and *M. stellae* Pennesi & Poulin in size and shape of the valve and the bilobed partecta. Differs in the shape and arrangement of the areolae from *M. ovulum* (Figs 56, 57), which has apically elongate areolae tending to form an irregular quincunx pattern and internal areolae not in longitudinal rows (Pennesi et al. 2013, table 1). Distinguished from *M. emarginata* (see above) in lacking the evident partectal pores and from *M. stellae* in the striae pattern and shape of the areolae (rectangular and sunken in contrast to round and flush).

Mastogloia obliqua Hagelstein Figs 62, 63
Ref. illus.: Hagelstein 1939, pl. 5, figs 12, 13; Giffen 1980, pl. 2, figs 23, 23a, 24; Loir & Novarino 2013, pl. 16c
Samples: **GU66F-4**
Dimensions: Length 13 µm, width 4.4 µm, striae *ca.* 25 in 10 µm.
Diagnostics: Small, rostrate valves with one partectum on each side (sometimes two, as shown by Hagelstein 1939), placed slightly obliquely across the central area.

Comments: Comparable with *M. tenuis* Hustedt (Lobban et al. 2012, pl. 37, figs 6–8), which is not rostrate, has finer striae, and has two small tapering partecta bordering the larger partecta on each side, the chambers symmetrically placed (as in most *Mastogloia* spp.) and also has axial costae bordering the internal raphe-sternum. Also similar to *M. giekesii* Cholnoky (Loir & Novarino 2013, pl. 13a), which is rostrate, has two chambers on each side (apparently never only one), symmetrically placed.

Mastogloia peracuta Janisch Figs 64–67
Section Decussatae
Ref. illus.: Hustedt 1931–1959, fig. 906; Ricard 1974, pl. 4(22), fig. 12; Montgomery 1978, pl. 132, figs E, F (as *Mastogloia rhomlus* [sic] (Petit) Cleve); Navarro 1983a, figs 52, 53; Yohn & Gibson 1992, figs 1–6; Hein et al. 2008, pl. 43, fig. 1; Loir & Novarino 2013, pl. 18a
Samples: **GU44AP-9**
Dimensions: Length 27–29 µm, width 14–16 µm; striae 17 in 10 µm.
Diagnostics: Rostrate valves with coarse, transapically elongate areolae in decussate pattern, with a band of smaller, square areolae along the margin. Raphe straight, central endings close together.
Comments: Our specimens do not entirely agree with Hustedt's (1931–1959) description, especially that the transapical length of their areolae does not gradually increase from the raphe to the margin and that the apical partecta, while wider than the others, are not twice the width. Nevertheless, it does match more recent descriptions and SEM observations (Yohn & Gibson 1982, Loir & Novarino 2013), with the exception of the external appearance of the areolae depicted by Paddock & Kemp (1990, fig. 44). Hustedt (1931–1959) contrasted it with the very similar *M. rhombus* (Petit) Cleve & Grove. In our flora it resembles *M. lacrimata* Voigt (Lobban et al. 2012, pl. 30, figs 6–8) in the large, decussate pattern of transapically elongate areolae, though in the latter the transapical striae are noticeably curved, and the partectal chambers readily distinguish it.

Mastogloia cf. *pumila* (Grunow) Cleve Figs 68–72
Section Sulcatae
Ref. illus.: Hustedt 1931–1959, fig. 983; Witkowski et al. 2000, pl. 83, figs 5, 6; Loir & Novarino 2013, pl. 19c
Sample: **GU52P-1, GU52P-9**
Dimensions: Length 10–17 µm, width 5.5–6.5 µm; striae 27 in 10 µm, radiate
Diagnostics: Small valves, elliptical-lanceolate with slightly rostrate apices; central area extended into an H-shaped hyaline area. In our small cells, 1–2 large partecta in the middle flanked by 1–2 tapering partecta on each side and the H-shaped hyaline area is not evident externally.
Comments: These small specimens have chambers much like *M. sergiana* Pennesi & Poulin (Lobban et al. 2012, pl. 36, figs 7, 8 and pl. 37 figs 1, 2), *M. manokwariensis* Cholnoky (Lobban et al. 2012, pl. 32, figs 1–3), *M. pusilla* var. *subcapitata* Hustedt (Hustedt 1931–1959, fig 1002e, Loir & Novarino 2013, pl. 20b), and *M. urveae* Witkowski, Lange-Bertalot & Metzeltin (Witkowski et al. 2000, pl. 84, figs 22, 23, Loir & Novarino 2013, pl. 24a, 27b). However, the elliptical valve outline and the distinct lyrate hyaline area distinguish it from each of these. *M. urveae* also differs in having parallel striae (Witkowski et al. 2000). Larger size ranges for *M. pumilla* were given by Hustedt (1931–1959) (20–20 x 5–9 µm) and Loir & Novarino (2013) (17.5–25 x 6.5–7.5 µm).

Mastogloia quinquecostata Grunow Figs 73–79
Section Sulcatae.
Ref. illus.: Peragallo & Peragallo 1897–1908, pl. 6, fig. 3; Hustedt 1931–1959, fig. 989; Ricard 1974, p. 3(21), fig. 7; Ricard 1975, figs 32–35; Paddock & Kemp 1990, fig. 20c; Witkowski et al. 2000, pl. 80, figs 7, 8
Samples: **GU44I-2, GU44K-6, GU52Q-10a, GU66A-5**, GU66F-8

Dimensions: Length 30–58 µm, width 14–19 µm; striae 22–24 in 10 µm
Diagnostics: Elliptical-lanceolate to rhombic-lanceolate valves with strong longitudinal lines and narrow partectal rings with square to apically rectangular partecta. Outer raphe is strongly sinuous and the inner straight; central endings straight.
Comments: The species name refers to the strong longitudinal lines, which mark the borders of the pseudoconopeum; a thin dark line marking the joint in the pseudoconopeum can sometimes be seen in LM and is clear in SEM (Figs 77, 78, arrows). Our stria densities are higher than those in Peragallo & Peragallo (1897–1908) (15–16 in 10 µm) and Hustedt (1931–1959) (16–20 in 10 µm). Montgomery (1978, pl. 138, figs A–E, pl. 139, figs C, D) has exterior SEMs labeled as *M. quinquecostata*, but they all show specimens with true conopea, open along the side, in contrast to Paddock & Kemp's (1990) illustration. The partecta shown in Witkowski et al. (2000) do not match those in Hustedt's (1931–1956) drawings.

Mastogloia seychellensis Grunow Figs 80–82
Section Paradoxae
Ref. illus.: Hustedt 1931–1959, fig. 958 ; Loir & Novarino 2013, pl. 21c
Samples: **GU52Q-10a**
Dimensions: Length 45–48 µm, width 13 µm; transapical striae 27 in 10 µm, longitudinal striae 26 in 10 µm.
Diagnostics: Elliptical-lanceolate valves with rostrate apices, the partecta strongly displaced toward the midline and with evident ducts leading obliquely to the valvocopula wall.
Comments: *M. seychellensis* is similar to *M. paradoxa* Grunow (Hustedt 1931–1959, fig. 953; in our flora: Lobban et al. 2012, pl. 34, figs 3–5) and *M. similis* Hustedt (Hustedt 1931–1959, fig. 954); the latter differs from *M. paradoxa* only in having a straight raphe. In these taxa the middle chambers are distinctly larger than the rest, instead of forming a graded series as in *M. seychellensis*, and both have axial costae along the raphe, which are absent from *M. seychellensis*. The size ranges of *M. seychellensis* and *M. paradoxa* are respectively 30–50 µm and 50–60 µm according to Hustedt. Although Hustedt showed the raphe of *M. seychellensis* as perfectly straight, the Guam specimens have a distinctly wavy raphe. On the strength of the difference Hustedt (1931–1959) used to erect *M. similis*, this would be enough to exclude these specimens from *M. seychellensis* but we do not yet have adequate material to address the differences among these species.

Nitzschia janischii Grunow Figs 83–88
Ref. illus.: Grunow 1880, pl. 13, fig. 14; Peragallo & Peragallo 1897–1908, pl. 76, fig. 14
Samples: **GU44Z-15, GU44AK-2, GU44AR-2**
Dimensions: Length 225–275 µm, width 7–9 µm; striae 23 in 10 µm; fibulae 4 in 10 µm
Diagnostics: Extremely long valves with irregularly spaced fibulae extending completely across the valve face. Central nodule present (Fig. 86). Areolae arranged in quincunx pattern of transapical and diagonal striae. Fourteen large, platelike plastids observed, with large pyrenoids (Fig. 83).
Comments: *N. janischii* is most similar to *Tryblionella scalaris* (Ehrenberg) Siver & Hamilton [= *N. scalaris* (Ehrenberg) W. Smith] (Ruck & Kociloek 2004, pl. 62–65), but that primarily freshwater/brackish species has ribs that extend only halfway across the valve face, besides the characters that make it *Tryblionella*. *N. janischii* was not recorded from The Bahamas (Hein et al. 2008), Puerto Rico (Hagelstein 1939, Navarro 1983b), Mahé (Giffen 1980), or Tahiti (Ricard 1977), and we are aware of no record other than Grunow's. No ultrastructure images are cited in Gaul et al. (1993) or Henderson & Reimer (2003). Grunow (1880) illustrated only half of a specimen from the Hawaiian Islands, where it was "rare," but Peragallo & Peragallo (1897–1908) drew a whole valve; it is not clear whether they saw Grunow's specimen, as they mention it only as a "curious exotic form," perhaps not in the French flora. Grunow placed his species in Section

Epithemioides, rather than Subgenus *Denticula*, but the differences are ill-defined. *Denticula* is now regarded as a separate genus, and Round et al. (1990, p. 622) commented that *Denticula* is, "Closely related to *Nitzschia* sect. *Grunowia*, from which it is difficult to separate, except on the extent of the fibulae." In *Denticula* all the fibulae "extend across the valve face, forming partitions running from margin to margin. The fibulae widen at their bases (near the raphe) so that only small apertures ('portulae') are left connecting cell interior with subraphe canal." This is also true of *N. janischii*, yet fibulae reaching the valve margin is not a synapomorphy for *Denticula* because a few other *Nitzschia* species also have this character, e.g., *N. rhopalodioides* Hustedt (Hustedt 1955, p. 45, pl.15, fig. 16), and even *N. ventricosa* Kitton (Lobban et al. 2012, pl. 61, figs 1, 2), although there, as in *Gomphonitzschia clevei* Grunow (Grunow 1880, pl. 14, fig. 11, Peragallo & Peragallo 1897–1908, pl. 76, fig. 15), some extend only part way and some costae extend part way back from the margin. At present there does not seem to be justification for reclassifying *N. janischii* in *Denticula*.

Nitzschia nienhuisii F.A.S. Sterrenburg & F.J.G. Sterrenburg Figs 89–94
Ref. illus: Sterrenburg & Sterrenburg 1990, figs 2–4; Hein et al. 2008, pl. 59, figs 2, 3
Samples: GU7R; **GU44AY-6; GU52P-1**
Dimensions: Length 49–53 µm, width 16 µm; striae not resolved, even in SEM.
Diagnostics: Hyaline cells with protracted apices, the raphe raised on a keel, both branches curving to the same side.
Comments: This species is very similar to a hyaline *Entomoneis* in our flora, but is distinguished by the raphe branches curving to the same side, whereas those of *Entomoneis* are sigmoid (curve to opposite sides). The *Entomoneis* is also larger. When valves are acid cleaned the membranous valve collapses. There do not appear to be fibulae on the keel in the usual sense of them in *Nitzschia*, and Sterrenburg & Sterrenburg (1990) assigned this species to the genus with hesitation. There are markings on the keel, but these in SEM appear to be nothing more than wrinkles in the membranous valve material. The structure of this species is baffling but may be resolved with TEM.

Petroneis humerosa (Brébisson ex W. Smith) Stickle & D.G. Mann Figs 95–97
Ref. illus.: Peragallo & Peragallo 1897–1908, pl. 27, fig. 20; Hustedt 1961–1966, fig. 1702 (both as *Navicula humerosa*); Witkowski et al. 2000, pl. 101, figs 2, 3, pl. 102, fig. 3
Samples: **GU44I-3**
Dimensions: Length 45–60 µm, width 29–34 µm; striae 12 in 10 µm
Diagnostics: Valves broad, linear, slightly rostrate. Strongly radiating striae with coarse areolae; short striae interspersed between longer ones along the central linear part of the valve.
Comments: Similar to *P. latissima* Gregory and *P. monilifera* Cleve (Hustedt 1961–1966, figs 1701, 1699), but those have coarser striae. There are a number of small ultrastructural differences between *Petroneis* and *Cosmioneis* which together warranted their separation (Round et al. 1990: 526); SEMs from a sample in the Davis collection from Saipan, CNMI (Figs 96, 97), show the internal central raphe endings to be crozier- rather than anchor-shaped, suggesting that the Guam specimen is also *Petroneis*. However, *C. delawariensis* (Grunow ex Cleve) D.G. Mann (Witkowski et al. 2000, pl. 106, figs 1, 2) is very similar in LM.

Pinnunavis yarrensis (Grunow) H. Okuno Figs 98–105
Syn.: *Pinnularia yarrensis* (Grunow) Jurilj, *Navicula yarrensis* Grunow
Naviculales: Naviculaceae.
Ref. illus.: Grunow in Schmidt et al. 1874–1959, pl. 46, figs 1–6; Meister 1932, pl. 17, fig. 139; Hustedt 1955, pl. 9, fig. 2; Navarro 1983a, figs 108–110; Wah & Wee 1988, fig. 64 (all as *Navicula*

yarrensis); Witkowski et al. 2000, pl. 146, fig. 11; López-Fuerte et al. 2010, pl. 29, figs 1, 2 (both as *Pinnularia yarrensis*); Okuno, 1975, fig. 8-2 and 2a
Samples: GU69A-1
Dimensions: 36–105 µm long, 15–32 µm wide, 4–7 striae in 10 µm.
Diagnostics: Striae radiate along most of the valve but convergent at the apices. Striae consisting of single alveolus with numerous small poroids in the outer membrane and no inner membrane (Figs 102–104). The two plastids (Fig. 98) extend onto the valve face nearly to the raphe, with closely lobed margins. Valve shape varied from elliptical-lanceolate to linear with broadly rounded apices; size also varied widely in this population.
Comments: SEM views confirm the images shown by Navarro (1983a). I also noted that the inner margin of the valvocopula is scalloped to fit against the outer edges of the interstriae (Fig. 105). There is a single line of pores near the abvalvar edge of the wide valvocopula (Fig. 103).

A "striking species of massive sculpture" (Mann 1925:125), and equally handsome alive. This species is usually noted as widespread but scarce (Hustedt 1955:32; Witkowski et al. 2000:338), but was abundant in GU69A-1 from surface sediment at the edge of a mangrove. Navarro (1982a), Wah & Wee (1988) and López-Fuerte et al. (2010) also reported it from mangroves. Meister (1932:43) reported linear valves of the nominate variety from Cavite Bay, Luzon, Philippines (habitat not given). The number of striae reported varies from 3–3.5 in 10 µm (Meister 1932) and 4 in 10 µm (Witkowski et al. 2000), to 10 in 10 µm (Podzorski & Håkansson 1987); the more finely striate forms are not so readily distinguished from *Navicula.* In my sample, the smaller valves (Fig. 104) had denser striae but appear to still be the same species. Length range in the literature is 60–200 µm (Witkowski et al. 2000); the smallest valve I found was 36 µm long. Several varieties have been named, including three from Miocene deposits (Hajós 1968; California Academy of Sciences 2011). *Navicula yarrensis* was first transferred to *Pinnularia* (Jurilj 1957) and later to a new genus, *Pinnunavis* Okuno (1975), along with *P. elegans* (W. Smith) Okuno, and this is the currently accepted name for *P. yarrensis* according to AlgaeBase (Guiry & Guiry 2014). However, *Pinnunavis elegans* (W. Smith) Okuno was transferred back to *Pinnularia* by Krammer (1992). The plastids of *P. elegans* lie along the girdle bands, typical of *Navicula* and *Pinnularia* (A. Witkowski, personal communication), whereas those seen here for *P. yarrensis* spread across the valve face, more like those of some *Diploneis*. It remains to be seen how these genera are related molecularly.

Plagiogramma atomus Greville Fig. 106
Ref. illus.: Ricard 1977 pl. 10, fig. 10; Witkowski et al. pl. 3, figs 7, 8; Hein et al. 2008, pl. 4, figs 9,10
Samples: **GU44L-E**
Dimensions: Length 25–28 µm, width 13–14 µm; striae ca. 11 in 10 µm
Diagnostics: The bilobed outline together with the dimensions define this species.
Comments: Larger and more finely areolate than a more common, so far unidentified specimens close to *P. bilobatum*. Reported for Guam by Arai (2010, pl. 8, fig. 2).

Pogoneis bahrainii F.E. Round & P.W. Basson Figs 107–113
ORDER and Family *incertae sedis*
Ref. illus.: Round & Basson 1997, figs 1–3, 13–25
Samples: GU44I-4
Dimensions: 15–17 µm long, 2.3–2.7 µm wide; striae 45 in 10 µm (both valves).
Diagnostics: The monoraphid frustules are very distinctively shaped like a canoe in girdle view because of thickenings on raphe valve (RV) apices and the curvature of the sternum valve (SV).

Striae are parallel and comprise slits which are apically elongated on both valves, except diagonal near RV apices.
Comments: Dimensions and stria densities agree with Round & Basson's material from Bahrain. A slide from this sample with the holotype of *Cyclophora minor* (accession #627405, slide 223019) at California Academy of Sciences also has a marked specimen of *P. bahrainii*. The taxonomic position of this genus was not specified by Round & Basson (1997); as a monoraphid diatom it could have been placed in Achnanthales, but since Cox (2006) removed *Achnanthes* sensu stricto to Mastogloiales, there is no single order to which all monoraphid taxa belong.

Protokeelia cholnokyi (Giffen) F.E. Round & P.W. Basson Figs 114–117
RHOPALODIALES D.G. Mann: Rhopalodiaceae (Karsten) Topachevs'kyj & Oksiyuk
Ref. illus.: Giffen 1963, figs 27–29 (as *Auricula cholnokyi* Giffen); Round & Basson 1995a, figs 1–9.
Samples: **GU44I-1, GU44J-2, GU44Z-15**
Dimensions: Length 16–19 µm, depth (from ventral corners to apex of dorsal curve) 10–14 µm; striae ca. 18 in 10 µm, measured transversally across striae near the ventral margin.
Diagnostics: Dorsal (convex) margin nearly circular to weakly reniform; two distinct indentations on the dorsal side of the valve. A ridge (or fold) on the ventral side of the valve arises from points that are not clearly indented and curves closer to the dorsal than the ventral margin. Spines absent.
Comments: The genus *Protokeelia* was established by Reimer & Lee (1984) for an endosymbiotic diatom isolated from a foram, and subsequently three new free-living species were described by Round (1993) and Round & Basson (1994, 1995b), all from Bahrain and neighboring Saudi Arabia. The literature was reviewed by Round & Basson (1995a), who re-examined *Auricula cholnokyi* and transferred it and *A. quinquelobata* Voigt to *Protokeelia*, so there are now six species. Although Round & Basson (1995b) wrote that "each new site visited seems to yield a new species," no further reports of new species have been published in the last 20 years; however, it seems unlikely that the biodiversity of *Protokeelia* has been exhausted, particularly elsewhere in warm waters. The known species have all been epipelic; the specimens we have seen were collected in algal turfs but these samples typically contain sediment.

The terminology is somewhat confusing, because the valve shows only one side as usually lying with the raphe on a ridge along the convex (dorsal) margin and the ventral margin more or less concave. The side thus showing is the ventral part of the valve, while the dorsal part is narrower and has the indentations (clearly seen in the whole frustule SEM, Fig. 117). The distinction between *P. cholnokyi* and *P. quinquelobata* has not been examined in SEM, but Round & Basson (1995a) assert that "the shape of the valve and of the ridge on the ventral face" suggest the two species are distinct. Voigt's (1960, pl. 2, figs 8, 9, 10) taxon is more reniform and the ventral ridge arises and curves closer to the ventral margin than is the case in *P. cholnokyi.* Reexamination of Voigt's material is needed to verify the distinction. The taxon given in Witkowski et al. (2000, p. 410, pl. 215, figs 11, 12) as "*Protokeelia cholnokyana* (Giffen) Round et Basson" is described as "narrowly reniform" and is much shallower than specimens illustrated by Giffen and Round & Basson.

***Psammodictyon pustulatum* (Voigt ex Meister) Lobban, n. comb., n. stat.** Figs 118–128
Basionym: *Nitzschia panduriformis* var. *pustulata* Voigt ex Meister 1937, Berichte der Schweizerischen Botanischen Gesellschaft 47: 270, pl. 11, fig. 9.
Samples: **GU66A-1, GU66A-3, GU66F-2, GU66F-7A; GU52Q-10**
Dimensions: Length 22–33 µm, width 13–17 µm; striae 20–24 in 10 µm, fibulae ca. 14 in 10 µm.
Diagnostics: Differs from all other species of *Psammodictyon* in the presence of a pair of rounded elevations on the distal side of the sternum.

Description: Valves panduriform, highly sculptured, with a pair of rounded elevations on the distal side of the sternum and a pair of shallow depressions on the proximal side. Valves apiculate and loculate; areolae in quincunx arrangement, the striae interrupted by a hyaline sternum near the mid line (Figs 123, 124). (The part next to the raphe is considered proximal, and the side toward the mantle where the elevations occur is distal.) The raphe system is submarginal, dividing the valve into a wide ventral portion and a narrow dorsal band; pores on the dorsal portion consist of a longitudinal row of transapical slits (Figs 127, 128: arrows). The dorsal part of the valvocopula has a repand *ab*valvar edge (Figs 124, 125). The distal part of the ventral valve face bears two rounded elevations; the proximal portion slopes down from the raphe-keel to the sternum in two shallow depressions (Figs 125, 126, 128). Loculae are evident on the elevations (Figs 125, 126) but also can be seen on the proximal side of the sternum (Fig. 125). Girdle bands lack pores, except for a single longitudinal row on the first pleura (Fig. 125: arrow). The valvocopula delimits the ventral margin of the valve with a repand rim and there is a single row of pores at its base on the valve side (Figs 125, 126); however, along the dorsal portion of the valvocopula, the opposite edge is repand (Figs 124, 125).

Comments: The loculate structure places this taxon in *Psammodictyon* rather than *Nitzschia* or *Tryblionella*; the character combinations distinguishing these genera are described by Round et al. (1990). However, the valve face is sharply delimited by a vertical rim, which appears to be formed by the valvocopula, rather than merging imperceptibly into a shallow mantle on the ventral side, as described by Round et al. (1990) for *Psammodictyon*. The possibility that this rim is simply due to collapse of the frustule during preparation is unlikely because of the consistency of its appearance in the SEM images and the way it goes down under the dorsal margin (Figs 127, 128).

I examined Meister's slide 3509092, and found one specimen—apparently not the type he photographed, however, since it is partially overlain by another diatom (Fig. 121).

Although Meister (1937) in the same paper also named *Nitzschia pustulata*, this is entirely different and certainly not a *Psammodictyon*, so I am confident there will be no future confusion from using *pustulatum* as the epithet in this new combination.

Specimens labeled as *N. panduriforme var. pustulata* occur on two slides in the Hustedt collection (ZT2/46 and W1/18), kindly photographed by Friedel Hinz (one shown in Fig. 122), are identical to my specimens; a similar specimen is illustrated in Stidolph et al. (2012, pl. 25, fig. 83). The known geographic range of *P. pustulatum* is thus Nagasaki (Japan), Guam, Singapore, Galapagos, and Vera Cruz (Mexico).

The size and outline of *P. pustulatum* are similar to *P. constrictum* in our flora, but the areolae, with single pores on both sides, are like those in *P. panduriforme,* unlike those in *P. constrictum,* where there are complex external openings and clusters of 3–4 interior pores. Further differences in *P. constrictum* are that the areolae on the dorsal side of the raphe-keel are also large, and the pleura has transapical striae all along it (Lobban et al. 2012, pl. 59, figs 7, 8).

Pteroncola marina Holmes & Croll Figs 129, 130

FRAGILARIALES Silva: Fragilariaceae Greville

Ref. illus.: Holmes & Croll 1984, figs 2–15; Round et al. 1990, pp. 390–391, figs a–i

Samples: GU41D-A1; Jordan plankton tow Talofofo; black mangrove roots at Merizo (coll. Shiori Tamura)

Dimensions: Length 5.3–8.4 µm, width 2.6 µm; striae 75 in 10 µm

Diagnostics: Small tabulate frustules; exceedingly fine striae consist of very closely spaced pores (smaller than the apical pores); apical pores aligned conspicuously at 90° to the striae, as seen in girdle view. Thickened spots along edge of valve mantle.

Comments: The striae are alveolate, opening internally by single pores (Round et al. 1990), as in *Caloneis* and *Oestrupia*; Fig. 130 is consistent with this, and the pores can be seen through the external areolae. Round et al. (1990) proposed synonymy of *P. marina* and *P. inane* (Giffen) F.E.

Round (*Dimerogramma inane* Giffen 1970a, figs 20–22), which has elevated apices, but re-examination of Giffen's materials in LM and SEM (A. Witkowski, personal communication) showed that *P. marina* is distinct. Almandoz et al. (2014) described a new species, *P. carlinii* Almandoz & Ferrario with much different striae, and also emended the genus description.

Rhoiconeis pagoensis **Lobban n. sp.** Figs 131–138
NAVICULALES Bessey: Naviculaceae Kützing
Samples: GU7X-2, GU7X-7
Dimensions: Length 16–49 μm, width 6.7–7.9 μm; striae 16–22 in 10 μm
Diagnosis: Differing from the other two species in the stria density.
Holotype: Slide # 1319 from GU7X-7, Fig. 133. Deposited at California Academy of Sciences, accession # 627426 slide # 220342.
Type locality: Pago Bay, Guam, 13°25'40" N, 144°47'57" E, on shore in University of Guam Marine Laboratory seawater outfall stream, collected by C. Lobban, 3 June 2013.
Paratypes: Slides #1265, 1266, 1270–1272 in UOG Diatom Herbarium.
Etymology: named for the type locality, Pago Bay, itself probably from *pagu*, the Chamorro name for the tree *Hibiscus tiliaceus* L., whose bark was traditionally used to make rope.
Description: Live cells motile, two plastids lying along the girdle faces as in *Navicula* (Fig. 131, 132). Frustules flexed in girdle view, the central areas of the two usually different, with the broader area on the concave side (Figs 136, 137). Striae lineate, radiate except for short ones bordering the central area (Figs 135, 137). Valvocopula in two segments, with a sigmoid junction near one apex (Fig. 138); the smaller segment reminiscent of the end plate in *Rhabdonema arcuata* (Pocock & Cox 1982). There were slight differences in stria count common between apices and center, the two apices and the two valves. Frustules did not come apart even after double acid cleaning and I was not able to get SEM of the internal valve face.
Comments: Samples were collected over several days from a diatom bloom in an outfall stream from the U. Guam Marine Laboratory seawater system. The bloom developed soon after the seawater flow was restarted, epiphytic on a population of the siphonous green alga *Trichosolen* sp., itself known to be rare except for blooming after a major disturbance (Lobban & Tsuda 2003).

Rhoiconeis Grunow was resurrected by Medlin (1985) and currently includes two species (Table 1). The genus is characterized by naviculoid frustules flexed in girdle view and having lineate striae and internal siliceous sheets joining the outer parts of the interstriae. There is a distinctive pattern in the girdle bands, with a segmented valvocopula and two pleural bands, as shown in Medlin (1985, fig. 38; compare with my Fig. 138). In *Rhoiconeis* both valves are raphid, in contrast to *Achnanthes*; isopolar, in contrast to *Rhoicosphenia*; and distinguished from *Campylopyxis* by the pores, girdle bands, and internal valve features. Both known species of *Rhoiconeis* have radiate, lineate striae and slightly different central areas on the convex and concave valves. Thus, the present material can be positively identified as *Rhoiconeis* even without good internal views, and can be distinguished from the other species on the basis of valve size and stria density (Table 1).

Rhoicosigma compactum (Greville) Grunow Figs 139–143
Ref. illus.: Van Heurck 1896, pl. 28, fig. 802; Peragallo & Peragallo 1897–1908, pl. 35, fig. 8
Sample GU52N-7, GU52O-3; **GU52P-1**
Dimensions: Length 97–118 μm, width 16–23 μm, striae 20–22 in 10 μm.
Diagnostics: Frustule bent along the valvar plane (achnanthoid) (Fig. 139); raphe on concave/ventral valve highly sigmoid, the other (convex valve) nearly straight (as for the genus) (Figs 140, 141, 143). Plastids are several large plates (Fig. 139). Central raphe endings overlap on both valves (Fig. 142).

Table 1. Comparison of *Rhoiconeis* species.

Character	***R. bolleana* (Grunow) Medlin**	***R. sponsalia* (Giffen) Medlin**	***R. pagoensis* n. sp.**
Length (µm)	40–60 [45–95][a]	20–42	16–49
Width (µm)	9–10 [10–11][a]	5–7.5	6.7–7.9 (only 2 samples)
Striae in 10 µm	8–11 at center, denser at apices	13–15, consistent throughout	16–22
Stria angle	Radiate throughout, more strongly towards apices	Radiate throughout	Radiate throughout
Central area	On concave valve quadrate, 3–5 shorter striae; on convex elliptical, 1–3 short striae	On concave valve quadrate, 3–4 shorter striae; on convex elliptical, fewer short striae	Both valves 2–5 short striae, both can have quadrate central area, narrow area seen only on convex valve.
Plastids	unknown	unknown	Two plates, lying along girdle faces
Girdle bands	unknown	valvocopula and pleura in 2 parts	valvocopula and pleura in 2 parts

[a] Numbers in brackets from Cleve (1895), others from Medlin (1985).

Comments: Hein & Lobban (2015) included two SEMs of this species for comparison with their new species *R. parvum*. Here I present full documentation of the record. Peragallo & Peragallo (1897–1908) gave length = 77–180 µm, whereas Van Heurck (1896) gave rather larger dimensions of 140–180 x 35 µm, both gave stria density of 20–24 in 10 µm for *R. compactum*. *R. oceanicum* H. Peragallo (Peragallo & Peragallo 1897–1908, pl. 35, figs 3–7) is still larger (160–260 x 36–45µm), with still coarser striae (17–18 in 10 µm). Hendey (1964, p. 250) gives dimensions of *R. compactum* as 90–150 µm, transapical striae 17–20 in 10 µm, longitudinal striae 22–24 in 10 µm, but he cites Peragallo & Peragallo (1897–1908) figs 3, 4, 6, 7 and 8, whereas their figs 3–7 are identified as *R. oceanicum*.

Seminavis robusta Danielidis & D.G. Mann Figs 144, 145
Syn.: *Seminavis ventricosa* (Gregory) M. Garcia-Baptista; *Amphora ventricosa* Gregory
Ref. illus.: Hendey 1964, pl. 38, fig. 12 (as *Amphora ventricosa*); Navarro 1982b, fig. 16 (as *Amphora angusta* var. *ventricosa*); Danielidis & Mann 2002, figs 39–53; Wachnicka & Gaiser 2007, figs 221–225; Hein et al. 2008, pl. 57, figs 3, 5; John 2012, figs 125 A–J, 126 A, B (as *Seminavis ventricosa*); Stidolph et al. 2012, pl. 24, fig. 73 (as *Amphora angusta* var. *ventricosa*)
Samples: **GU52Q-1a, GU52Q-10a**
Dimensions: Length 65–74 µm, width 13–14 µm; dorsal striae strongly radiate at the center, 13–16 in 10 µm, less radiate toward the apices, 15–18 in 10 µm; ventral striae radiate at center, 14 in 10 µm, parallel toward apices, 16–18 in 10 µm.
Diagnostics: Semi-lanceolate valves, the raphe closer to the ventral side. Axial area asymmetrical, wider on the dorsal side (the hyaline areas seen in SEM to be grooves).
Comments: Differs from other (as yet unidentified) *Seminavis* spp. in our flora in the size and coarse striation. The most similar species is *S. latior* (A. Schmidt) Danielidis & D.G. Mann (2002, figs 35–41, and see Wachnicka & Gaiser 2007, figs 226, 227), in which the striae are uniformly spaced throughout, both 13–15 in 10 µm, and the ventral striae are radiate throughout, rather than parallel toward the apices. The width of our specimens matches the range given by Danielidis &

Mann (2003) for *S. latior* and not *S. robusta*, but the range given by Wachnicka & Gaiser (2007) encompasses our broader specimens. More clearly distinct are *S. basilica* Danielidis (Danielidis & Mann 2003, figs 1–19), which has denser (19–25 in 10 µm), parallel striae throughout on both ventral and dorsal surfaces, and *S. insignis* Álvarez-Blanco & S. Blanco (2014), 20–26 dorsal striae in 10 µm.

Surirella cf. *fastuosa* Ehrenberg, *sensu* Ruck & Kociolek 2004 Figs 146–149
Ref. illus.: Ruck & Kociolek 2004, pl. 11–13
Samples: **GU44L-C, GU44AQ-1, GU44AQ-3, GU44AR-1, GU66A-2, GU66C-7, GU66F-4**
Dimensions: Length 62–81 µm, width 39–45 µm. Infundibula 2.5 in 10 µm.
Diagnostics: Broadly oval, the sides nearly straight, sometimes very weakly indented; neither the valve margin nor the keel markedly constricted or convex at the center. Lanceolate central area (circlet) with external ribs, but lacking short striae on the perimeter; puncta completely absent on internal side of circlet.
Comments: Plastids: two lobed plates, as in typical *Surirella fastuosa* (Fig. 146). Larger, more oval, and more symmetrical than *S. fastuosa*, and without the short striae on the circlet. These specimens match the California sample described by Ruck & Kociolek (2004), except for the complete lack of puncta on the inner face of the circlet here. Ruck & Kociolek identified their material only as comparable to *S. fastuosa* "until such time as the type material is examined and the variability in morphology documented." Given this situation, I list this taxon as separate from *S. fastuosa.*

Amendments and corrections to previous lists

A list of significant corrections to Lobban et al. (2012) was posted on the *Micronesica* website[2] and printed on p. 280 of the hardcopy when that was finally released in October 2013. Of particular note is that *Pleurosigma intermedium* is for now removed from the flora. Sterrenburg pointed out several ultrastructural features in which our material differs (see Sar et al. 2012); his summary is posted on our ProtistCentral website at http://www.protistcentral.org/Photo/get/photo_id/2912. We also corrected our error in referring to ***Mastogloia sergiana* Pennesi & Poulin** as *Mastogloia sergensis.* Also, as noted above, I correct the identity of the valve in pl. 68, fig. 4 to *Campylodiscus fastuosus* and substituted a correct images on the web page for *Surirella scalaris*.

I correct our name for the record of *Nitzschia constricta* (Gregory) Grunow to ***Psammodictyon constrictum* (Gregory) D.G. Mann** on the basis of the loculate valves.

A nomenclatural change that came to my attention since Lobban et al. (2012) went to press is Reid's (2012) change of *Donkinia minuta* to ***Carinasigma minuta* (Donkin) G. Reid**. The areolae in our specimens are arranged in transverse and longitudinal rows, consistent with this new genus (SEM in Jordan et al. 2009–2015: http://www.protistcentral.org/Photo/get/photo_id/4537). More recently, *Lyrella hennedyi* var. *granulata* was promoted to ***L. granulata* (Grunow) Nevrova, Witkowski, Kulikovskiy & Lange-Berthalot** (Nevrova et al. 2014).

Finally, one taxonomic change affects a species reported from Yap by Navarro & Lobban (2009): ***Conticribra weissflogii* (Grunow) K. Stachura-Suchoples & D.M. Williams** is the new name for *Thalassiosira weissflogii* (Grunow) G. Fryxell & Hasle (Statchura-Suchoples & Williams 2009).

[2] http://micronesica.org/sites/default/files/12_lobban_et_al_2012_errata.pdf

Discussion

Several of the new records and one of the new species have come from samples that were not from farmer-fish territories and hint at the diversity in these other habitats. These include: (1) A mangrove mud surface dominated by *Pinnunavis yarrrensis* (see above), *Carinasigma* sp., *Pleurosigma* sp., and *Navicula* sp., but also with an interesting *Petroneis* that may be a new species (http://www.protistcentral.org/Taxa/get/taxa_id/586006). (2) A diatom patch from a sand/turf mat in a very shallow (and warm) area close to shore on a reef flat, dominated by *Amphora rhombica* var. *intermedia* (see above), and *A. decussata*, with *Haslea* sp. (again, possibly new) and a variety of epiphytic species such as *Cocconeis scutellum* Ehrenberg, *Mastogloia fimbriata* (Brightwell) Cleve, and *Gato hyalinus* Lobban & Navarro. (3) A diatom bloom on seaweeds in a newly re-started seawater outfall stream at UOG Marine Laboratory, dominated by *Podosira baldjickiana* Grunow, *Donkinia* sp., *Melosira* sp., *Licmophora* aff. *ehrenbergii*, *Psammodictyon constrictum*, *Actinocyclus tenuissimus* Cleve, and *Pleurosigma* sp. and including *Rhoiconeis pagoensis* (see above).

While *Psammodictyon pustulatum* is distinctive, there are many small panduriform nitzschioid taxa in our flora. Most common is *Psammodictyon constrictum* (images of some odd ones at http://www.protistcentral.org/Taxa/get/taxa_id/585923). We have also observed the characteristic lateral, asymmetrical plastids of *Psammodictyon* in field material (http://www.protistcentral.org/Photo/get/photo_id/3650) but have not linked live cells with any of the valve types seen in SEM. Second, there is an interesting connection with the endosymbiotic diatoms in forams; forams are abundant and diverse in Guam (Richardson & Clayshulte 2003). One of the endosymbionts is *P. panduriforme* var. *continuum* (Grunow) Snoejis (=*N. panduriformis* var. *continua* Grunow), a variety similar in size to the just taxa mentioned, found in forams from the Red Sea (Lee et al. 1980a). Lee et al.'s (1980a, figs 16, 17) illustrations of it are strikingly like *P. constrictum*, and not like nominate *P. panduriforme*. It was the dominant diatom in Red Sea samples of *Heterostegina depressa* d'Orbigny (Lee et al. 1980a), but was replaced by *N. valdestriata* Aleem & Hustedt in Hawaiian samples of this foram (Lee et al.1980b), and the suite of diatom endosymbionts was different again on the Great Barrier Reef (Lee & Correia 2005). *H. depressa* also occurs on Guam (Richardson & Clayshulte 2003) and it would be interesting to see what species is present here. As far as we can tell from these images, the Red Sea endosymbiont is indistinguishable from specimens we are calling *P. constrictum*. However, as Witkowski et al. (2000), among others, have noted, the whole complex around this group of species needs a general taxonomic revision, and that must include gene sequencing. Lee (2011) summarized the occurrences of endosymbiotic diatoms in forams thus: "Less than two dozen species of diatoms are involved in the phenomenon. All are small (≤10 µm). *Nitzschia frustulum* var. *symbiotica* is the most common species. This species along with two other species of *Nitzschia*, *N. laevis* Hustedt and *N. panduriformis* var. *continua* Grunow in Cleve and Grunow, *Nanofrustulum shiloi* (Lee, Reimer, and McEnery) [Round, Hallenstein & Paasche], *Amphora roettgerii* Lee and Reimer, and *Amphora erezii* Reimer and Lee, were isolated from over 75% of the associations." To date we have found free living *N. shiloi* in Guam (Navarro & Lobban 2009).

These records add another 8 *Mastogloia* taxa to the 55 previously listed. In comparison, Martinez-Goss & Evangelista (2010, 2011) listed 86 taxa for the Philippines. Loir & Novarino (2013) reported 90 taxa (72 identified to species) from sandy sediments around three islands in the French Antilles (Caribbean), and noted that only 19 of those occurred on all three islands. In comparing our list with theirs, 38 taxa (52%) we have identified are also in their list of identified species; this is similar to the fractions we found when comparing our total checklist with lists for several other sites (Lobban et al. 2012).

The taxa reported here bring the total published records for Guam to 271. A great many taxa remain to be identified from those already documented, much additional study of samples in the collection is needed, and many habitats remain to be sampled. New records will be added to the ProtistCentral website. As part of the ongoing project, the image bank, already >76,000 images, is being developed into a herbarium collections database that can eventually become a public resource.

Acknowledgements

The microscopes used at U. Guam were funded by NIGMS RISE award GM063682 and US Dept. Education MSEIP award P120A040092. I thank María Schefter for continuous support and encouragement with the diatom research, the Commanding Officers of Naval Base Guam for access to study sites there, and Matt Ashworth for many helpful discussions and especially for assistance with the SEMs at U. Texas and the identity of *Pogoneis*. Thanks to Lukas Taxböck for assistance with Meister's slides and notes, and to the Institute of Systematic Botany, U. Zurich for loan of the slides. I am grateful to Friedel Hinz at Diatomeenforschung, Alfred-Wegener-Institut, Helmholtz-Zentrum für Polar- und Meeresforschung, for photographing specimens on two slides in the Hustedt collection, including those in Figs 121 and 122, and for the photo of Voigt's figure with a ruler, to Elizabeth Ruck for the images in Figs 115 and 117, and to Ric Jordan and Misaki Ishizawa for Fig. 130.

References

Al-Kandari, M., F.Y. Al-Yamani & K. Al-Rifaie. 2009. Marine Phytoplankton Atlas of Kuwait's Waters. Kuwait Institute for Scientific Research, Safat, Kuwait. 350 pp.

Almandoz, G.O., M.E. Ferrario, M.J. Sullivan, L. Ector & I.R. Schloss. 2014. A new *Pteroncola* species (Bacillariophyceae) from the South Shetland Islands, Antarctica. Phycologia 53: 188–194.

Álvarez-Blanco, I. & S. Blanco. 2014. Benthic diatoms from Mediterranean coasts. Bibliotheca Diatomologica 60: 1–409.

Arai, Y. 2010. Attached diatoms communities in farmer-fish territories. M.S. Thesis, Dept. of Earth and Environmental Sciences, Yamagata University, Japan.

California Academy of Sciences. 2011. Catalogue of diatom names, on-line version updated 19 Sept. 2011. Compiled by Elisabeth Fourtanier & J. Patrick Kociolek. Available online at http://research.calacademy.org/research/diatoms/names/index.asp. Accessed 22 June 2014.

Choi, J.K. & J.H. Noh. 1987. The fine structure of new recorded pennate diatoms in Korea. Korean Journal of Phycology 2: 97–117.

Cleve, P.T. 1895. Synopsis of the naviculoid diatoms. Kongliga Svenska Vetenskaps-Academiens Handlingar 26: 1–264.

Cox, E.J. 2006. *Achnanthes* sensu stricto belongs with genera of the Mastogloiales rather than with other monoraphid diatoms. European Journal of Phycology 41: 67–81.

Cupp, E.E. 1943. Marine plankton diatoms of the west coast of North America. Bulletin of Scripps Institution of Oceanography, Technical Series 5: 1–238.

Danielidis D.B. & D.G. Mann. 2002. The systematics of *Seminavis* (Bacillariophyta): the lost identities of *Amphora angusta*, *A. ventricosa*, and *A. macilenta*. European Journal of Phycology 37: 429–448.

Danielidis, D.B. & D.G. Mann. 2003. New species and new combinations in the genus *Seminavis* (Bacillariophyta). Diatom Research 18: 21–39.

De Stefano, M. & O.E. Romero. 2005. A survey of alveolate species of the diatom genus *Cocconeis* (Ehr.) with remarks on the new section *Alveolatae*. Bibliotheca Diatomologica 52: 1–133.

Gaul, U., U. Geissler, M. Henderson, R. Mahoney & C.W. Reimer. 1993. Bibliography on the fine structure of diatom frustules (Bacillariphyceae). Proceedings of the Academy of Natural Sciences Philadelphia 144: 69–238.

Giffen, M.H. 1963. Contributions to the diatom flora of South Africa I. Diatoms of the Estuaries of the Eastern Cape Province. Hydrobiologia 21: 201–265.

Giffen, M.H. 1970a. New and interesting marine and littoral diatoms from Sea Point, near Cape Town, South Africa. Botanica Marina 13: 87–99.

Giffen, M.H. 1970b. Contributions to the diatom flora of South Africa. IV. The marine littoral diatoms of the estuary of the Kowie River, Port Alfred, Cape Province. Beihefte zur Nova Hedwigia 31: 259–213, 5 pl.

Giffen, M.H. 1980. A checklist of marine littoral diatoms from Mahé, Seychelles Islands. Bacillaria 3: 129–159.

Gregory, W. 1857. On new forms of marine Diatomaceæ, found in the Firth of Clyde and in Loch Fine. Transactions of the Royal Society of Edinburgh 21: 473–542, pls. 9–14.

Grunow, A. 1880. On some new species of *Nitzschia* (with notes by Kitton). Journal of the Royal Microscopical Society, series 3, 3: 394–397, pl. 12–13.

Guiry, M.D. & G.M. Guiry2014. AlgaeBase. World-wide electronic publication, National University of Ireland, Galway. http://www.algaebase.org; accessed 22 Dec. 2013.

Güttinger, W. 1989. Collection of SEM-micrographs of Diatoms. Series 1–3. 150 plates. (Available from Koeltz Scientific Books, Koenigstein)

Güttinger, W. 1994. Collection of SEM-micrographs of Diatoms. Series 7. 50 plates. (Available from Koeltz Scientific Books, Koenigstein)

Hagelstein, R. 1939. Botany of Porto Rico and the Virgin Islands. Diatomaceae. New York Academy of Sciences, Scientific Survey of Porto Rico and the Virgin Islands, 8: 313–450.

Hajós, M. 1968 Mátraalja Miocén Üledékeinek Diatomái [Die diatomeen der Miozänen Ablagerungen des Mátravorlandes]. Geologica Hungarica, Series Paleontologica, Institutum Geologicum Hungaricum, Budapestini 37: 1–401.

Harwood, D.M. & T. Maruyama. 1992. Middle Eocene to Pleistocene diatom biostratigraphy of Southern Ocean sediments from the Kerguelen Plateau, Leg 120. *In* Wise, S. W., Schlich, et al. (eds.), Proceedings of the Ocean Drilling Program, Scientific Results. College station, Texas (Ocean Drilling Program) 120: 683–733.

Hasle, G. R. 1974. Some marine plankton genera of the diatom family Thalassiosiraceae. Beihefte zur Nova Hedwigia 45: 1–49.

Hein, M.K. & C.S. Lobban. 2015. *Rhoicosigma parvum* n. sp., a benthic marine diatom from the Bahamas and Western Pacific. Diatom Research 30: 75–85.

Hein, M.K., B.M. Winsborough & M.J. Sullivan. 2008. Bacillariophyta (diatoms) of the Bahamas. Iconographia Diatomologica 19. Gantner Verlag, Ruggell, Germany.

Henderson, M.V. & C.W. Reimer. 2003. Bibliography on the Fine Structure of Diatom Frustules (Bacillariophyceae). II. Gantner Verlag, Ruggell, Germany. 372 pp.

Hendey, N.I. 1964. An Introductory Account of the Smaller Algae of British Coastal Waters. Part V. Bacillariophyceae (Diatoms). Her Majesty's Stationery Office, London.

Hernández-Becerril, D. U. 1991. The morphology and taxonomy of species of the diatom genus *Asteromphalus* Ehr. Bibliotheca Diatomologica 23: 1–57 + 33 pl.

Holmes, R.W. & D.A. Croll. 1984. Initial observations on the composition of dense diatom growths on the body feathers of three species of diving seabirds. *In* D.G. Mann (ed.) Proceedings of the 7th International Diatom Symposium, pp. 265–277. Koeltz, Koenigstein, Germany.

Hustedt, F. 1927–1930. Die Kieselalgen Deutschlands, Österreichs und der Schweiz. *In,* Rabenhorst's Kryptogamenflora, Band 7, Teil 1. Johnson Reprint, New York.

Hustedt, F. 1931–1959. Die Kieselalgen Deutschlands, Österreichs und der Schweiz. *In,* Rabenhorst's Kryptogamenflora, Band 7, Teil 2. Johnson Reprint, New York.

Hustedt, F. 1961–1966. Die Kieselalgen Deutschlands, Österreichs und der Schweiz. *In* Rabenhorst's Kryptogamenflora, Band 7, Teil 3. Johnson Reprint, New York.

Hustedt, F. 1955. Marine Littoral Diatoms of Beaufort, North Carolina. Duke University Press. Durham, North Carolina. 67 pp.

John, J. 2012. Diatoms in the Swan River Estuary, Western Australia. Taxonomy and Ecology. Koeltz, Königstein, Germany.

Jordan, R.W., C.S. Lobban & E.C. Theriot. 2009–2015. Western Pacific diatoms project. ProtistCentral. http://www.protistcentral.org/index.php/Project/get/project_id/17.

Jurilj, A. 1957. Dijatomeje samatskog mora okoline Zagreba. (Flora of Diatoms of Sarmatic Sea in Environs of Zagreb). Jugoslavenska Akademija Znanosti i Umjetnosi, Zagreb. (Acta Biologica 1) 28: 5–153, 40 pls.

Krammer, K. 1992. *Pinnularia*. Eine Monographie der europäischen Taxa. Bibliotheca Diatomologica. 26: 1–353. J. Cramer. Berlin-Stuttgart.

Lee, J.J. 2011. Diatoms as endosymbionts. *In* J. Seckbach & J.P. Kociolek (eds), The Diatom World. [Cellular Origin, Life in Extreme Habitats and Astrobiology, vol. 19], pp. 437–464. Springer, Dordrecht, The Netherlands.

Lee, J.J. & M. Correia. 2005. Endosymbiotic diatoms from previously unsampled habitats. Symbiosis 38: 251–260.

Lee, J.J., C.W. Reimer & M.E. McEnery. 1980a. The identification of diatoms isolated as endosymbionts from larger Foraminifera from the Gulf of Eilat (Red Sea) and the description of 2 new species, *Fragilaria shiloi* sp. nov. and *Navicula reissii* sp. nov. Botanica Marina 23: 41–48.

Lee, J.J., M.E. McEnery, R. Röttger & C.W. Reimer. 1980b. The isolation, culture and identification of endosymbiotic diatoms from *Heterostegina depressa* d'Orbigny and *Amphistegina lessonii* d'Orbigny (larger foraminfera) from Hawaii. Botanica Marina 23: 297–302.

Lobban, C.S. & M.P. Ashworth. 2014a. *Hanicella moenia*, gen. et sp. nov., a ribbon-forming diatom (Bacillariophyta) with complex girdle bands, compared to *Microtabella interrupta* and *Rhabdonema* cf. *adriaticum*: implications for Striatellales, Rhabdonematales and Grammatophoraceae, fam. nov. Journal of Phycology 50: 860–884.

Lobban, C.S. & M.P. Ashworth. 2014b. *Lucanicum concatenatum*, n. gen., n. sp., a benthic marine diatom from Guam, and a less restrictive diagnosis for Cyclophorales (Bacillariophyta). Marine Biodiversity Records 7, e90, 8 pp. doi:10.1017/S1755267214000918.

Lobban, C.S. & R.W. Jordan. 2010. Diatoms on coral reefs and in tropical marine lakes. *In* J.P. Smol & E.F. Stoermer (eds), The Diatoms: Applications for the Environmental and Earth Sciences (2nd ed.). Cambridge University Press, Cambridge, U.K., pp. 346–356.

Lobban, C.S. & M. Schefter. 2013. *Licmophora comnavmaria* sp. nov. (Licmophorales, Bacillariophyta), a new diatom with intercalary rimoportulae. Marine Biodiversity Records 6: e109, 6 pp.

Lobban, C.S. & R.T. Tsuda. 2003. Revised checklist of benthic marine macroalgae and seagrasses of Guam and Micronesia. Micronesica 35-36: 54–99.

Lobban, C. S., M. Schefter, R.W. Jordan, Y. Arai, A. Sasaki, E.C. Theriot, M. Ashworth, E.C. Ruck & C. Pennesi. 2012. Coral-reef diatoms (Bacillariophyta) from Guam: new records and preliminary checklist, with emphasis on epiphytic species from farmer-fish territories. Micronesica 43: 237–479. [Errata on page 480 of the print edition and posted online at http://micronesica.org/sites/default/files/12_lobban_et_al_2012_errata.pdf]

Loir, M. & G. Novarino. 2013. Marine *Mastogloia* Thwaites ex W. Sm. and *Stigmaphora* Wallich specices from the French Lesser Antilles. Diatom Monographs 16: 1–133.

López Fuerte, F.O., D.A. Siqueiros Beltrones & J.N. Navarro. 2010. Benthic Diatoms Associated with Mangrove Environments in the Northwest Region of México. CONABIO, Gobierno Federal Méxicano, Mexico City. ISBN 978-607-7607-30-4.

Mann, A. 1925. Marine diatoms of the Philippine Islands. Smithsonian Institution Bulletin 100, 6(1): 1–182 + 39 pl.

Martinez-Goss, M.R & L.T. Evangelista. 2010. A check-list of *Mastogloia* (class Bacillariophyceae) of the Philippines. Philippine Journal of Science 139: 207–217.

Martinez-Goss, M.R & L.T. Evangelista. 2011. A contribution to the taxonomy of *Mastogloia* (Class Bacillariophyceae) in the Philippines. Philippine Journal of Science 140: 7–12.

Medlin, L.K. 1985. A reappraisal of the diatom genus *Rhoiconeis* and the description of *Campylopyxis*, gen. nov. British Phycological Journal 20: 313–328.

Meister, F. 1932. Kieselalgen aus Asien. Gebrüder Borntraeger, Berlin.

Meister, F. 1937. Seltene und neue Kieselalgen. II. Berichte der Schweizerischen Botanischen Gesellschaft 47: 258-276; pls. 3-13.

Montgomery, R.T. 1978. Environmental and Ecological Studies of the Diatom Communities Associated with the Coral Reefs of the Florida Keys. Volumes I and II. Ph.D. Dissertation, Florida State University, Tallahassee.

Navarro, J.N. 1982a. Marine diatoms associated with mangrove prop roots in the Indian River, Florida, U.S.A. Bibliotheca Phycologica 61: 1–151.

Navarro, J.N. 1982b. A survey of the marine diatoms of Puerto Rico. V. Suborder Raphidineae: Families Achnanthaceae and Naviculaceae (excluding *Navicula* and *Mastogloia*). Botanica Marina 25: 321–338.

Navarro, J.N. 1983a. A survey of the marine diatoms of Puerto Rico. VI. Suborder Raphidineae: Family Naviculaceae (Genera *Haslea*, *Mastogloia* and *Navicula*). Botanica Marina 26: 119–136.

Navarro, J.N. 1983b. A survey of the marine diatoms of Puerto Rico. VII. Suborder Raphidineae: Families Auriculaceae, Epithemiaceae, Nitzschiaceae and Surirellaceae. Botanica Marina 26: 393–408.

Navarro J.N. & C.S. Lobban. 2009. Freshwater and marine diatoms from the western Pacific islands of Yap and Guam, with notes on some diatoms in damselfish territories. Diatom Research 24: 123–157.

Nevrova, E., A. Witkowski, M. Kulikovskiy, H. Lange-Bertalot & J.P. Kociolek. 2014. A revision of the diatom genus *Lyrella* Karayeva (Bacillariophyta: Lyrellaceae) from the Black Sea, with descriptions of five new species. Phytotaxa 83: 1–38.

Okuno, H. 1975. The fine structure of the frustules of the Bacillariophyta. *In* J. Tokida & H. Hirose (eds), Advance of Phycology in Japan. Junk. The Hague. pp. 97-113.

Paddock, T.B.B. & K.D. Kemp. 1990. An illustrated survey of the morphological features of the diatom genus *Mastogloia.* Diatom Research 5: 73–103.

Paddock, T.B.B. & P.A. Sims. 1980. Observations on the marine diatom genus *Auricula* and two new genera *Undatella* and *Proboscidea*. Bacillaria 3: 161–196.

Pennesi, C., M. Poulin, F. Hinz, T. Romagnoli, M de Stefano & C. Totti. Comparison of two new species of *Mastogloia* (Bacillariophyceae) with other small members of section Ellipticae. Phytotaxa 126: 1–21.

Peragallo H. & M. Peragallo. 1897–1908. Diatomées Marines de France et des Districts Maritimes Voisins. M.J. Tempère, Grez-sur-Loing, France, pp. 491 + 137 pl.

Pocock, K.L. & E.J. Cox. 1982. Frustule structure in the diatom *Rhabdonema arcuatum* (Lyngb.) Kütz. with particular reference to the cingulum as seen with the scanning electron microscope. Nova Hedwigia 36: 621–641.

Podzorski, A.C. & H. Håkansson. 1987. Freshwater and marine diatoms from Palawan (a Philippine island). Bibliotheca Diatomologica 13: 1–245. J. Cramer, Berlin.

Reid, G. 2012. A revision of the family Pleurosigmataceae (Bacillariophyta). Diatom Monographs 14: 1–163.

Reimer, C.W. & J.J. Lee. 1984. A new pennate diatom: *Protokeelia hottingeri* gen. et sp. nov. Proceedings of the Academy of Natural Sciences, Philadelphia 136: 194–199.

Riaux-Gobin, C., O.E. Romero, P. Compère & A.Y. Al-Handel. 2011. Small-sized Achnanthales (Bacillariophyta) from coral sands off Mascarenes (Western Indian Ocean). Bibliotheca Diatomologica 57: 1–234.

Riaux-Gobin, C., P. Compère & L. Ector. 2014. Some *Cocconeis* species (Bacillariophyceae) originally described by William Gregory and Robert Kaye Greville from the Firth of Clyde and Loch Fyne (Scotland). Nova Hedwigia 99: 171–192.

Ricard, M. 1974. Etude taxonomique des diatomées marines du lagon de Vairao (Tahiti) 1. Le genre *Mastogloia.* Revue Algologique, nouvelle série 11: 161–177.

Ricard, M. 1975. Ultrastructure de quelques *Mastogloia* (diatomées benthiques) marines d'un lagon de Tahiti. Protistologica 11: 49–60.

Ricard, M. 1977. Les peuplements de diatomeés des lagons de l'Archipel de la Société (Polynésie Française). Revue Algologique, nouvelle série 12: 137–336.

Ricard, M. 1987. Atlas du Phytoplancton Marin. Vol. 2. Diatomées. Editions du CNRS, Paris.

Richardson, S.L. & R.N. Clayshulte. 2003. An annotated checklist of Foraminifera of Guam. Micronesica 35-36: 38–53.

Round, F.E. 1993. A new species of *Protokeelia*. Diatom Research 8: 203–207.

Round, F.E. & P.W. Basson. 1994. *Protokeelia spinifera* sp. nov., a benthic marine diatom from the Gulf coast of Saudi Arabia. Diatom Research 9: 155–163.

Round, F.E. & P.W. Basson. 1995a. The transference of *Auricula cholnokyi* Giffen and *A. quinquelobata* Voigt to *Protokeelia*. Diatom Research 10: 211–215.

Round, F.E. & P.W. Basson. 1995b. *Protokeelia aculeata* nov. sp. from Bahrain. Diatom Research 10: 333–339

Round, F.E. & P.W. Basson. 1997. A new monoraphid diatom genus (*Pogoneis*) from Bahrain and the transfer of previously described species *A. hungarica* and *A. taeniata* to new genera. Diatom Research 12: 71–81.

Round, F.E., R.M. Crawford & D.G. Mann. 1990. The Diatoms: Biology and Morphology of the Genera. Cambridge University Press, Cambridge, U.K., 747 pp.

Ruck, E.C. & J.P. Kociolek. 2004. Preliminary phylogeny of the family Surirellaceae (Bacillariophyta). Bibliotheca Diatomologica 50: 1–236.

Sar, E.A., F. Hinz, F.A.S. Sterrenburg, A.S. Lavigne, S. Lufeudo & I. Sunesen. 2012. Species of *Pleurosigma* (Pleurosigmataceae) with lanceolate or slightly sigmoid valve outlines: analysis of type material. Diatom Research 27: 237–253.

Schmidt, A. et al. 1874–1959. Atlas der Diatomaceen-Kunde. Series I–X. R. Reisland, Leipzig. (Reprint 1974 Koeltz, Koenigstein.)

Stachura-Suchoples, K. & D.M. Williams. 2009. Description of *Conticribra tricircularis*, a new genus and species of Thalassiosirales, with a discussion on its relationship to other continuous cribra species of *Thalassiosira* Cleve (Bacillariophyta) and its freshwater origin. European Journal of Phycology 44: 477–486.

Sterrenburg, F.A.S. & F.J.G. Sterrenburg. 1990. An outline of the marine littoral diatom biocoenosis of the Banc d'Arguin, Mauritania, West Africa. Botanica Marina 33: 459-465.

Stidolph, S.R., F.A.S. Sterrenburg, K.E.L. Smith & A. Kraberg. 2012. Stuart R. Stidolph Diatom Atlas: U.S. Geological Survey Open-File Report 2012–1163, available online at http://pubs.usgs.gov/of/2012/1163/ (accessed 25 July 2014).

Suzuki, H., T. Nagumo & J. Tanaka. 2008. Morphology and taxonomy of *Cocconeis subtilissima* Meister (Bacillariophyceae) and two closely related taxa from coastal waters of Japan. Journal of Japanese Botany 83: 269–279.

Syvertsen, E.E. & Hasle, G.R. 1982. The marine planktonic diatom *Lauderia annulata* Cleve, with particular reference to the processes. Bacillaria 5: 243–256.

Van Heurck, H. 1896. A Treatise on the Diatomaceae. William Wesley, London.

VanLandingham, S.L. 1968. Catalogue of the Fossil and Recent Genera and Species of Diatoms and their Synonyms. Part II. *Bacteriastrum* through *Coscinodiscus.* J. Cramer, Lehre.

Voigt, M. 1960. Note sur quelques diatomées du genre *Auricula*. Bulletin de l'Institut Royal des Sciences Naturelles de Belgique 36(2): 1–7, 2 pls.

Wachnicka, A. & E.E. Gaiser. 2007. Morphological characterization of *Amphora* and *Seminavis* (Bacillariophyceae) from South Florida, U.S.A. Diatom Research 22: 387–455.

Wah, T.T. & Y.C. Wee. 1988. Diatoms from mangrove environments of Singapore and southern peninsular Malaysia. Botanica Marina 31: 317–327.

Wallich, C.G. 1860. On the siliceous organisms found in the digestive cavities of the Salpae, and their relation to the flint nodules of the Chalk Formation. Transactions of the Microscopical Society of London, New Series 8: 36–55.

Williams, D.M. & G. Reid. 2006. Fossils and the tropics, the Eunotiaceae (Bacillariophyta) expanded: a new genus for the Upper Eocene fossil diatom *Eunotia reedii* and the recent tropical marine diatom *Amphora reichardtiana*. European Journal of Phycology 41: 147–154.

Williams, D.M. & G. Reid. 2009. New species in the genus *Colliculoamphora* Williams & Reid (Bacillariophyceae) with commentary on species concept in diatom taxonomy. Beihefte zur Nova Hedwigia 135: 185–199.

Witkowski A., H. Lange-Bertalot & D. Metzeltin. 2000. Diatom Flora of Marine Coasts, I. Gantner Verlag, Ruggell, Germany.

Yohn, T. A. & R.A. Gibson. 1982. Marine diatoms of the Bahamas. II. *Mastogloia* Thw. ex Wm. Sm. species of the groups Decussatae and Ellipticae. Botanica Marina 25: 41–53.

Received 03 August 2014, revised 12 January 2015.

PLATES

Figs 1–6. *Amphora rhombica* var. *intermedia* (GU43C). Figs 1, 2. Valve with curved raphe at two focal planes (DIC). Figs. 3, 4. Valve with nearly straight raphe at two focal planes (DIC). Fig. 5. Internal view of valve showing conopeum over central raphe endings (SEM). Fig. 6. External ventral view of valve showing girdle bands and conopeum over the central raphe endings. Fig. 7. *Asteromphalus cleveanus* (GU52N-4) (DIC). Figs 8, 9. *Asteromphalus hepactis* internal view and detail (GU56A) (SEM). Scale bars: Figs 1–4, 6–8 = 10 µm, Figs 5, 9 = 5 µm.

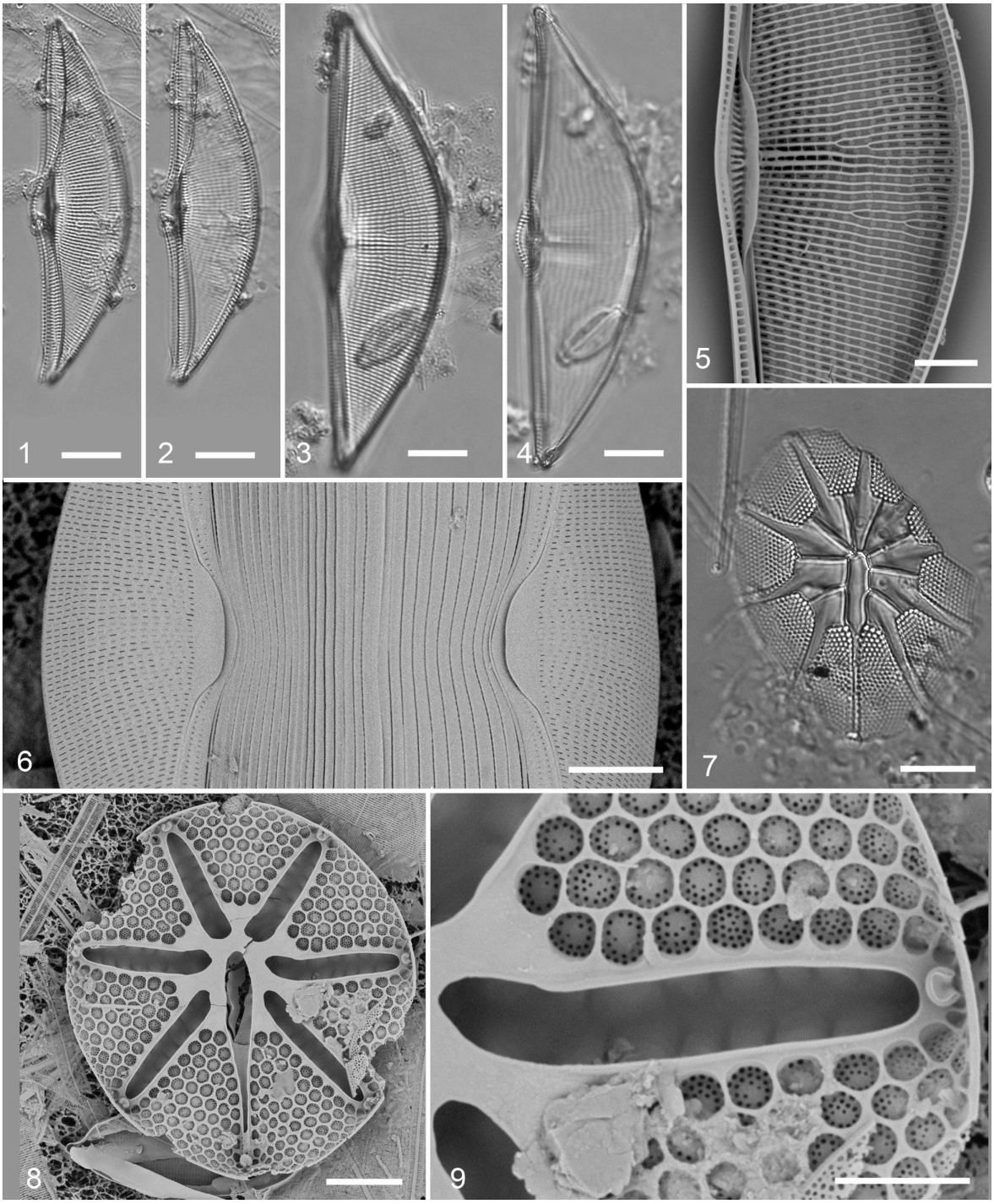
1
2
3
4
5
6
7
8
9

Figures 10–12. *Auricula flabelliformis*. Figs 10, 11. LM and SEM images of specimens from Yap (Y26B) (DIC) and Guam (GU66A-2) (SEM). Only half of each image is shown so that the delicate striation is visible. Fig. 12. Detail of internal valve face showing very short ventral surface and flabelliform striation (GU66A-2) (SEM). Fig. 13. *C. fastuosus* large valve (GU66F-8, catalog # GUD002914) (DIC). Figs 14, 15. *C. fastuosus* small valve (Fig. 14) compared to *S. scalaris* (GU52Q-2, GU52Q-10b respectively) (DIC). Scale bars: Figs 10, 11, 13–15 = 10 µm, Fig. 12 = 5 µm.

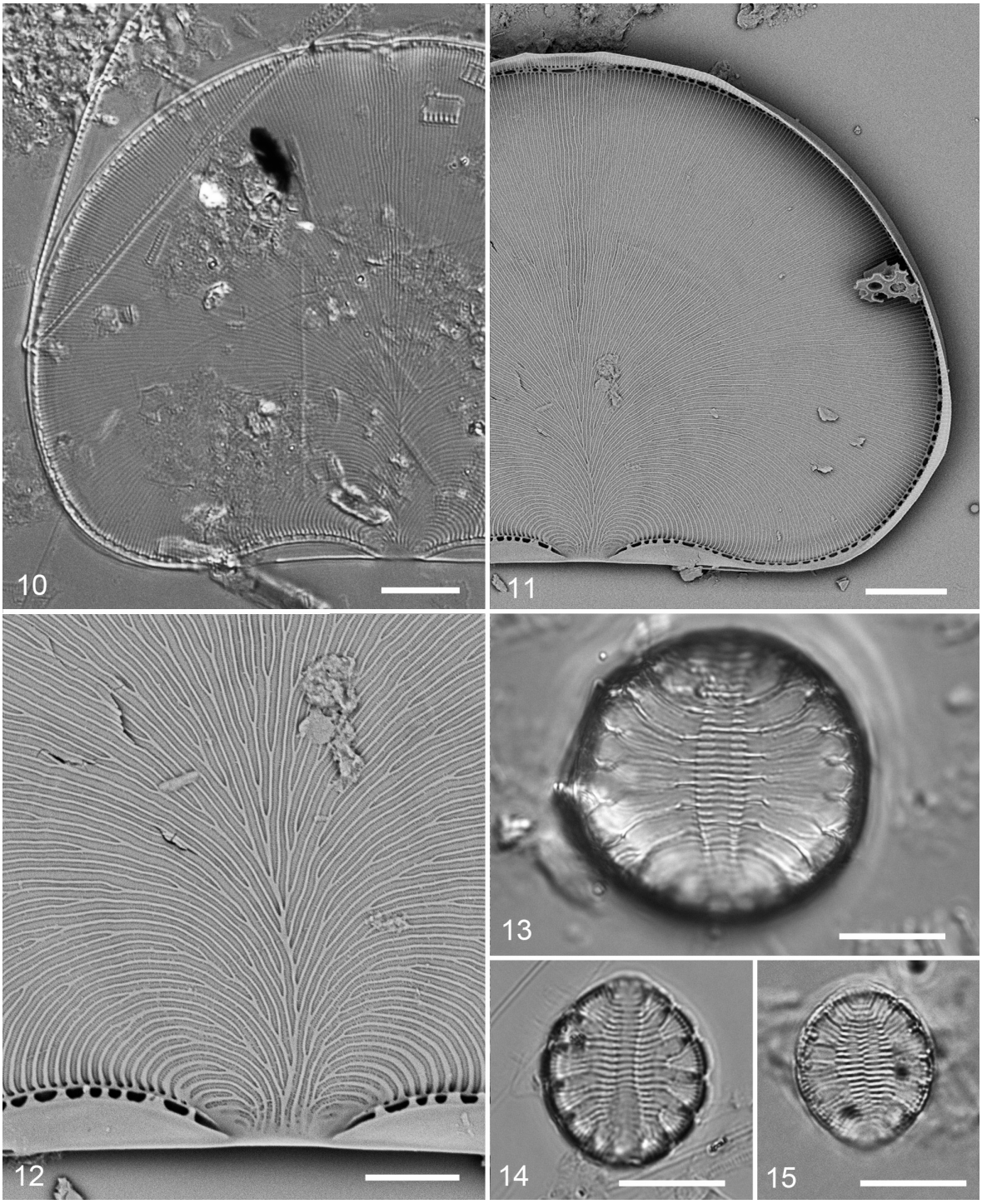
10
11
12
13
14
15

Figures 16–21. Figs 16, 17. Comparison of frustules of *Campylodiscus fastuosa* (Fig. 16) and *Surirella scalaris* (Fig. 17) showing crossed orientation of valves in the former versus parallel orientation in the latter. (GU66F-7A, GU52P-5, respectively) (SEM). Fig. 18. Frustule of *C. fastuosa* (GU66F-7A) (SEM). Figs 19, 20. *C. fastuosa* internal valves faces of small and large cells (GU66F-7A) (SEM). Fig. 21. *Cocconeis dapalistriata*, sternum valve (GU44AU-2) (SEM). Scale bars = 5 µm.

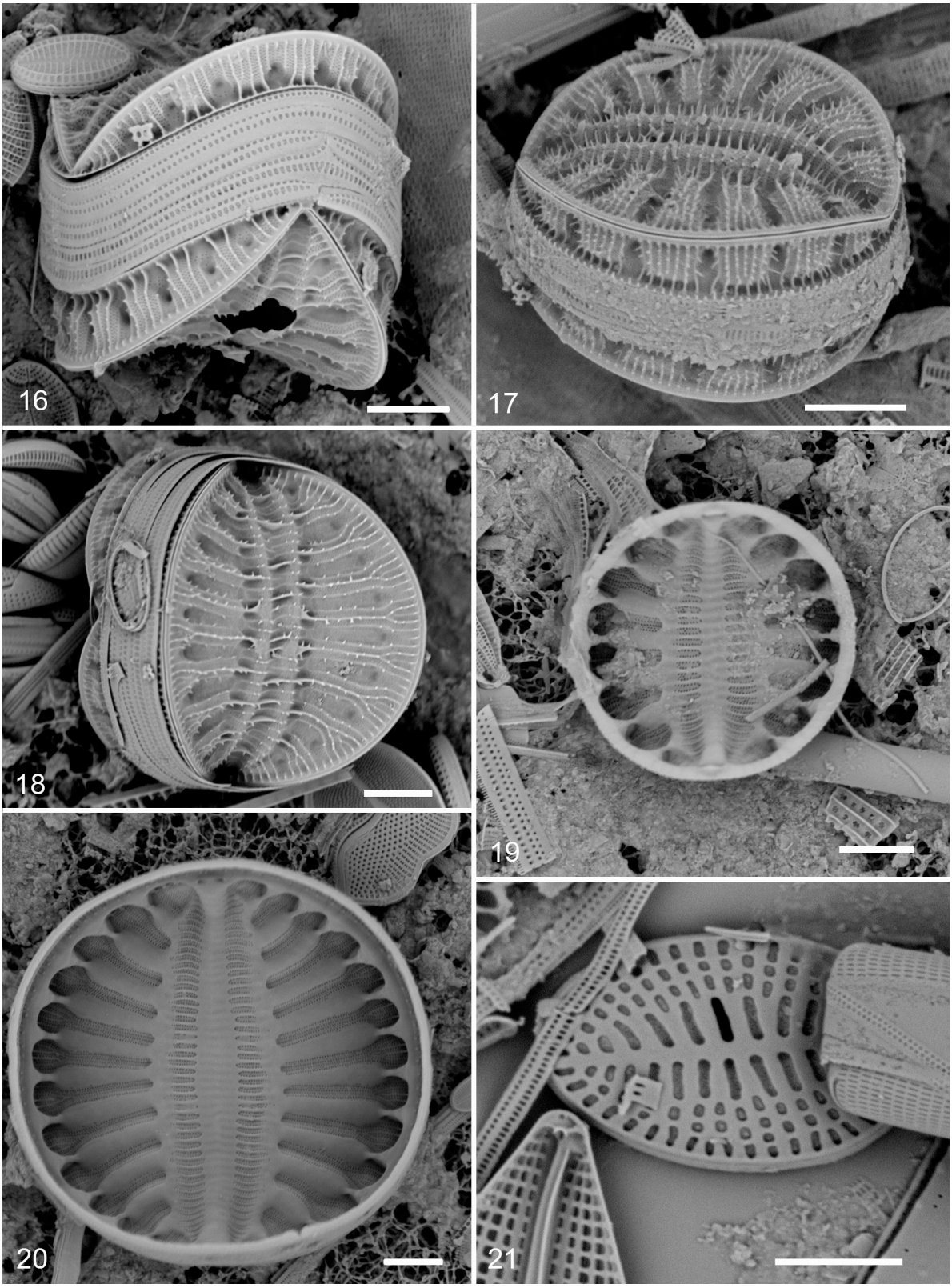
16
17
18
19
20
21

Figures 22–40. Figs 22–26. *Cocconeis ornata*, two valves at two focal planes each in DIC and external view in SEM (GU44AU-2). Figs 27–32. *Cocconeis subtilissima*. Figs 27, 28. Frustules in LM (GU44I-2, GU44Z-15) (DIC). Figs 29, 30. RV external and internal with valvocopula (GU44AQ-1). Figs 31, 32. SV external (whole mount, GU44AC-4), showing the alveolae at the fracture (arrow), and internal (GU44AQ-1). Figs 33–40. *Colliculoamphora gabgabensis*. Fig. 33. Holotype specimen (GU44AK-6) (DIC). Fig. 34. Paratype specimen (GU44I-1) (DIC). Fig. 35. Specimen showing deeper indentation (GU44AK-6). Figs 36–38. External views, showing the eunotid position of the raphe; arrows on Fig. 37 indicate short striae; Fig. 38 shows girdle bands (GU44AK-6, GU44Z-15, GU52Q-10a, respectively) (SEM). Figs 39, 40. Internal views (GU44W-10, GU44K-6) (SEM). Scale bars: Figs 22–36 = 5 µm, Figs 37, 38 = 2.5 µm, Figs 39, 40 = 2 µm.

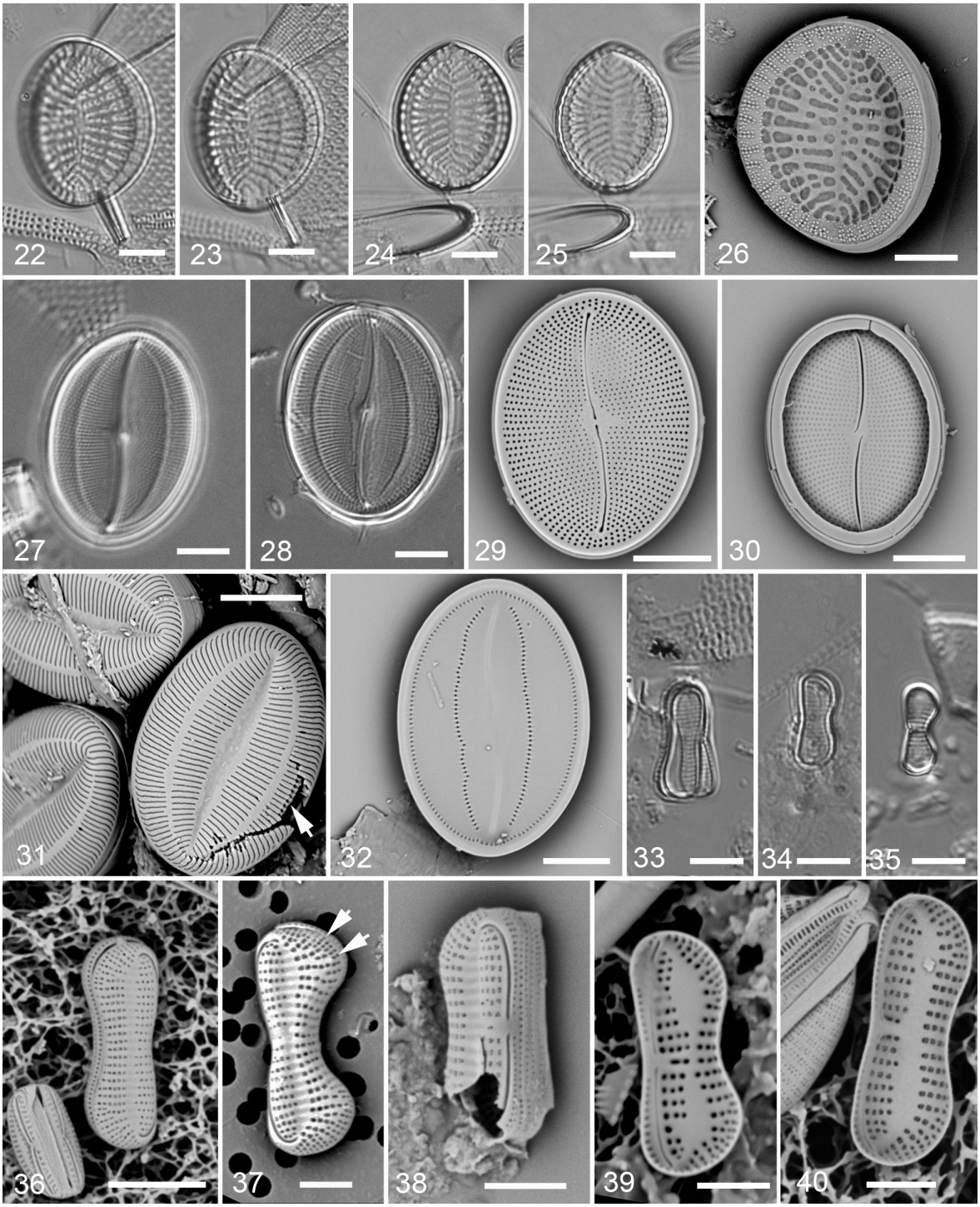
22
23
24
25
26
27
28
29
30
31
32
33
34
35
36
37
38
39
40

Figures 41–50. Figs 41, 42. *Hemidiscus cuneiformis* var. *ventricosa* (GU66F-4) (DIC). Fig. 41. Valve view; arrow points to pseudonodulus. Fig. 42. Oblique view with focus on several of the rimoportulae (arrow). Figs 43–48. *Lauderia excentrica*. Fig. 43. Holotype specimen (GU44I-1) (DIC). Fig. 44. External view of valve showing excentric, reniform annulus and external rimoportula opening (arrow) (GU44Y-13) (SEM). Fig. 45. External detail of annulus (GU55B-4) (SEM). Fig. 46. Internal view of valve with rimoportula (arrow), also showing the external aspect of the fultoportulae along the bottom rim (GY44Y-13) (SEM). Figs 47, 48. External and internal details of striae and fultoportulae, showing 5 satellite pores in the central fultoportulae (arrowhead) and 2-4 in the striae (arrow) (GU44Y-13) (SEM). Figs 49, 50. *Mastogloia affirmata* valve and valvocopula at two focal planes (GU44AX-1) (DIC). Scale bars: Figs 41, 42, 49, 50 = 10 µm, Figs 43, 44, 46 = 5 µm, Figs 45, 47, 48 = 2 µm.

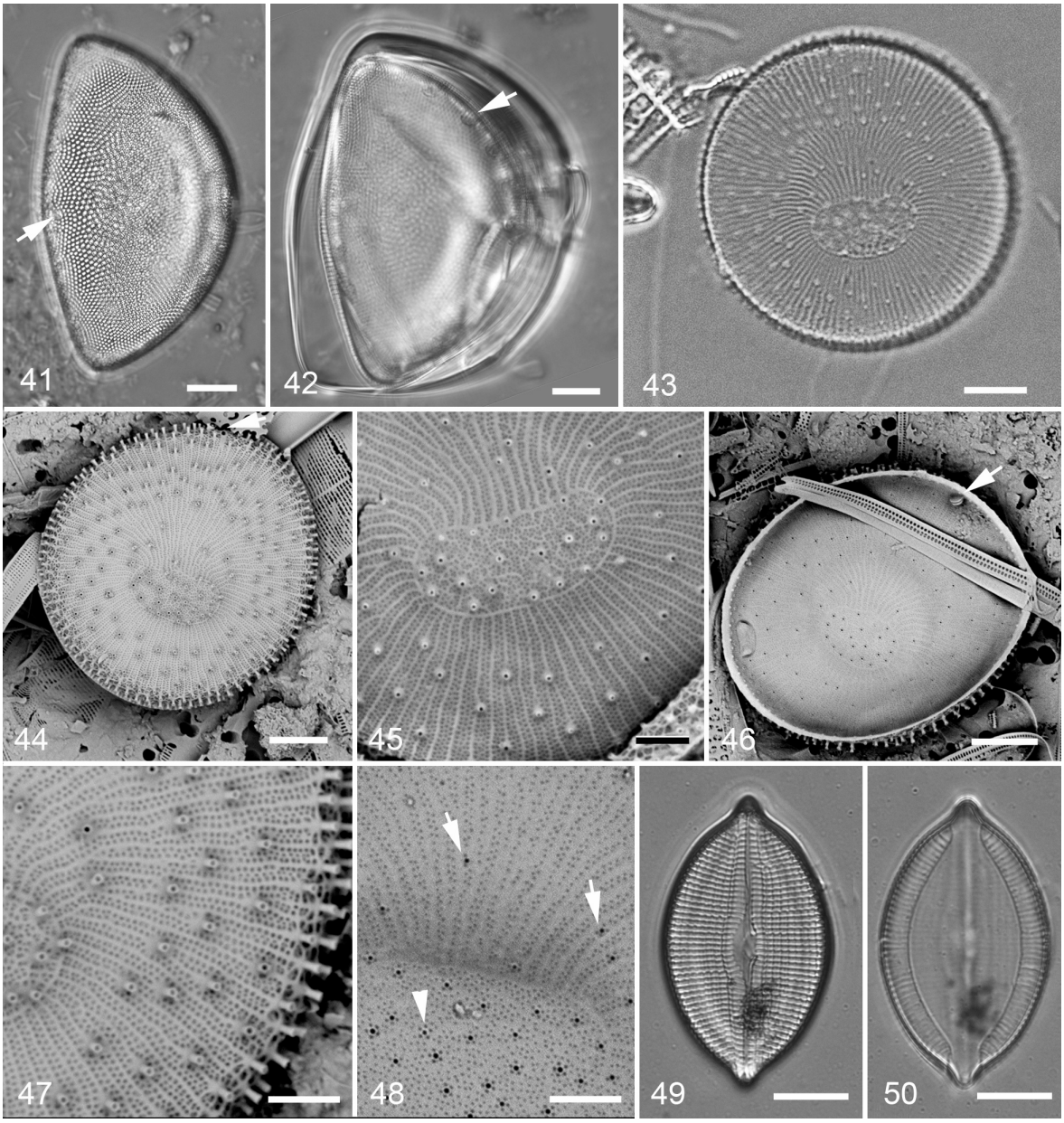
41
42
43
44
45
46
47
48
49
50

Figures 51–70. Figs. 51–55. *Mastogloia emarginata.* Figs 51-54. LM views of two specimens focused on valve face and valvocopula, arrowhead indicates one of the prominent exit pores of the partecta (GU44AR-2) (DIC). Fig. 55. Internal view of valve and valvocopula (GU55B-4) (SEM). Figs 56, 57. *Mastogloia ovulum* specimen at two focal planes (GU44K-6) (DIC). Figs 58-61. *Mastogloia matthaei*, two specimens at two focal planes (GU52P-2) (DIC). Figs. 62, 63. *Mastogloia obliqua*, valve at two focal planes (GU66F-4) (DIC). Figs. 64–67. *Mastogloia peracuta* (GU44AP-9). Figs 64, 65. Specimen at two focal planes (DIC). Figs 65, 66, External views of two specimens in SEM. Figs 68–71. *Mastogloia pumila*. Figs 68, 69. Specimen in DIC at two focal planes (GU52P-1; catalog # GUD002950). Fig. 70. Internal aspect of valve and valvocopula (GU52P-9) (SEM). Fig. 71. Frustule showing both internal and external valve faces. Scale bars: Figs 51–69 = 5 µm, Figs 70, 71 = 3 µm.

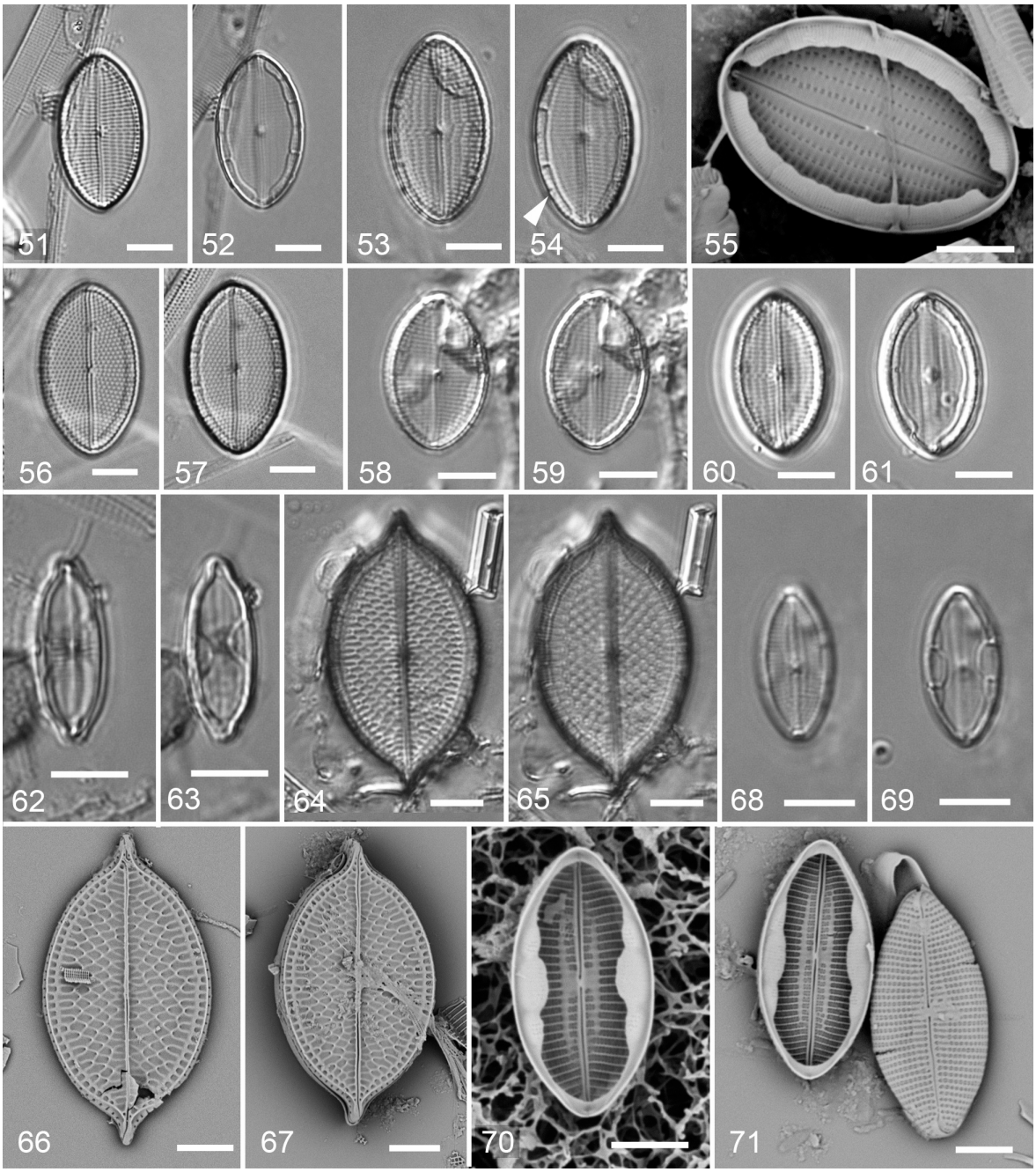
51
52
53
54
55
56
57
58
59
60
61
62
63
64
65
68
69
66
67
70
71

Figures 72–86. Fig. 72. *Mastogloia pumila*. Frustule showing two internal valve faces and valvocopulae; notice the variation in number of partecta (GU52P-1) (SEM). Figs 73–79. *Mastogloia quinquecostata*. Fig. 73. Live cell showing plastids (GU66A-5) (DIC). Figs 74–76. Frustule at three focal planes showing conopeum, areola pattern of valve face, and partecta (GU52Q-10a) (DIC). Figs 77, 78. Specimen at two focal planes showing the join in the conopeum (arrow) (GU44I-1) (DIC). Fig. 79. Oblique external view of valve showing seam along the conopeum (arrow) (GU66F-8) (SEM). Figs 80–82. *Mastogloia seychellensis* (GU52Q-10a). Figs 80, 81. Specimen at two focal planes, the valvocopula showing diagonal partectal ducts (DIC). Fig. 82. External view of valve (SEM). Figs 83–86. *Nitzschia janischii.* Fig. 83. Live cell in girdle view, showing nucleus (arrow) and plastids with pyrenoids (GU44AR-2) (DIC). Fig. 84. Portion of valve (GU44Z-15) (DIC). Figs 85, 86. Internal details of apex and central area, respectively, the latter showing the central nodule (arrow) (GU44AR-2) (SEM). Scale bars: Figs 73–78, 80–84 = 10 µm, Figs 72, 79, 85, 86 = 5 µm.

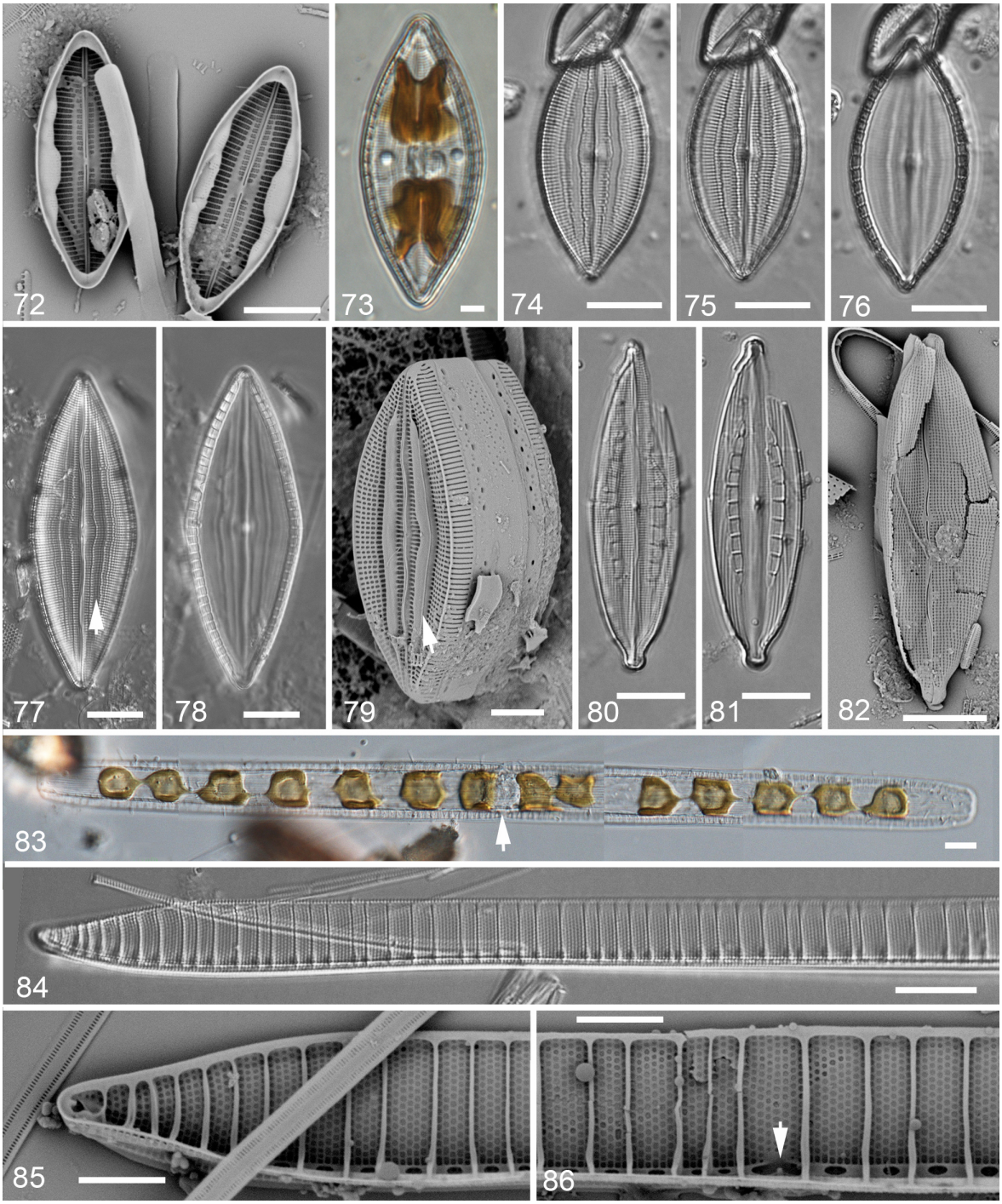
72
73
74
75
76
77
78
79
80
81
82
83
84
85
86

Figures 87–97. Figs 87, 88. *Nitzschia janischii* whole mount, details of central nodule and apex (GU44Z-15) (SEM). Figs 89–94. *Nitzschia nienhuisii.* Figs 89, 90. Girdle and valve views of the same cell in a wet mount (DIC). Figs 91, 92. Girdle and valve views of frustules in permanent mounts (GU44R-1, GU52P-1) (phase contrast). Figs 93, 94. Whole mount in SEM, and detail of central raphe endings (GU7R). Figs 95–97. *Petroneis humerosa* (GU44I-3). Fig. 95. Valve (DIC). Fig. 96. External view of valve (SEM). Fig. 97. Internal detail (SEM). Scale bars: Figs 87–93, 95, 96 = 10 µm, Fig. 94 = 2 µm, Fig. 97 = 5 µm.

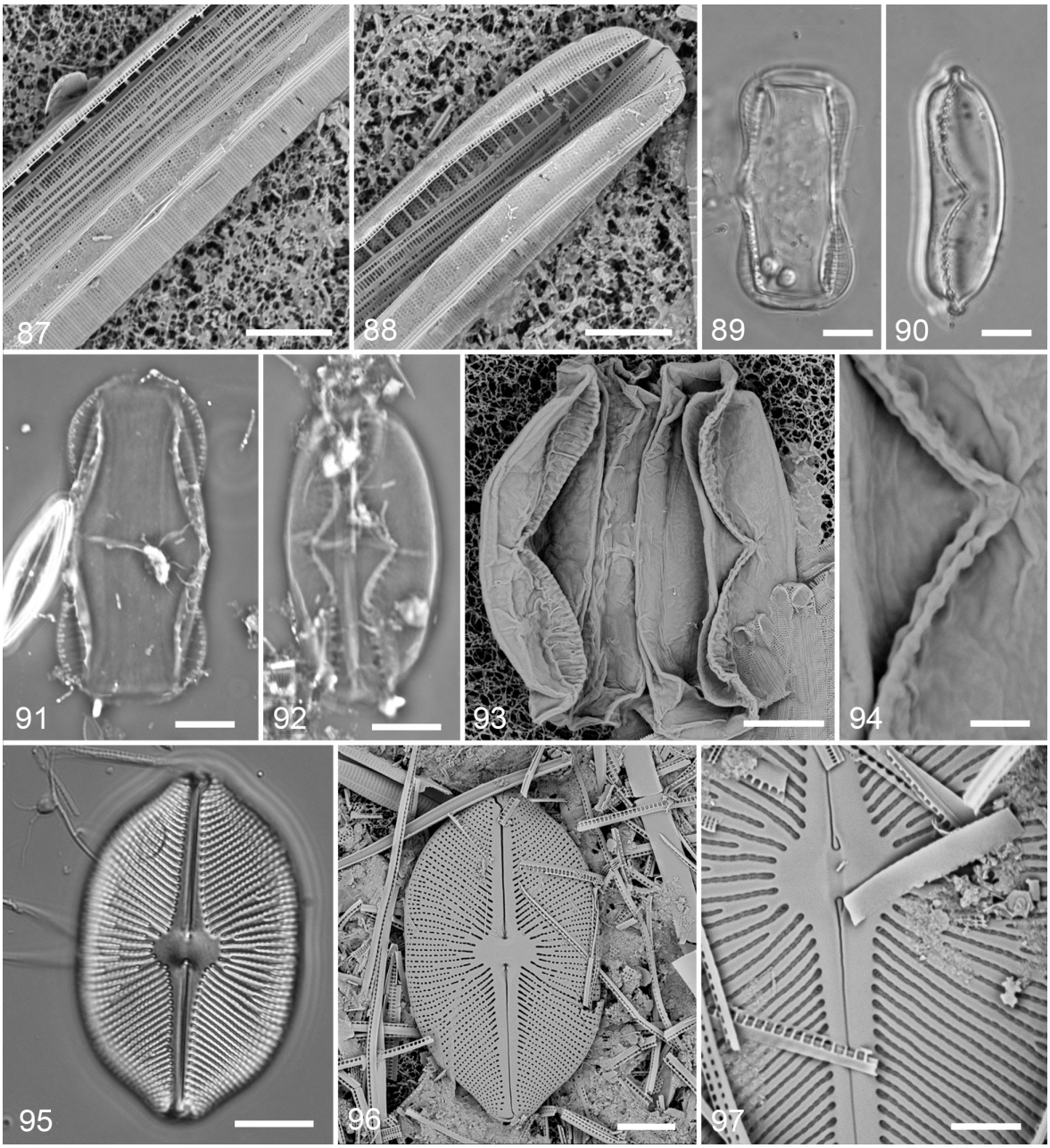
87
88
89
90
91
92
93
94
95
96
97

Figures 98–106. Figs 98–105. *Pinnunavis yarrensis* (GU69A-1). Fig. 98. Live cell showing plastid lobes below the valve surface (DIC). Figs 99–101. Three valves of different sizes (DIC). Fig. 102. Detail of areolae and central area, external (SEM). Fig. 103. Detail of girdle view showing valvocopula with single row of pores (SEM). Fig. 104. Fragment of apex, broken along the raphe slit, showing helictoglossa and thickened interstriae (SEM). Fig. Detail of valvocopula showing fluted margin of the pars interior (SEM). Fig. 106. *Plagiogramma atomus*, external valve view (GU44L-E) (SEM). Scale bars: Fig 98–101 = 10 µm, Figs 102–106 = 5 µm.

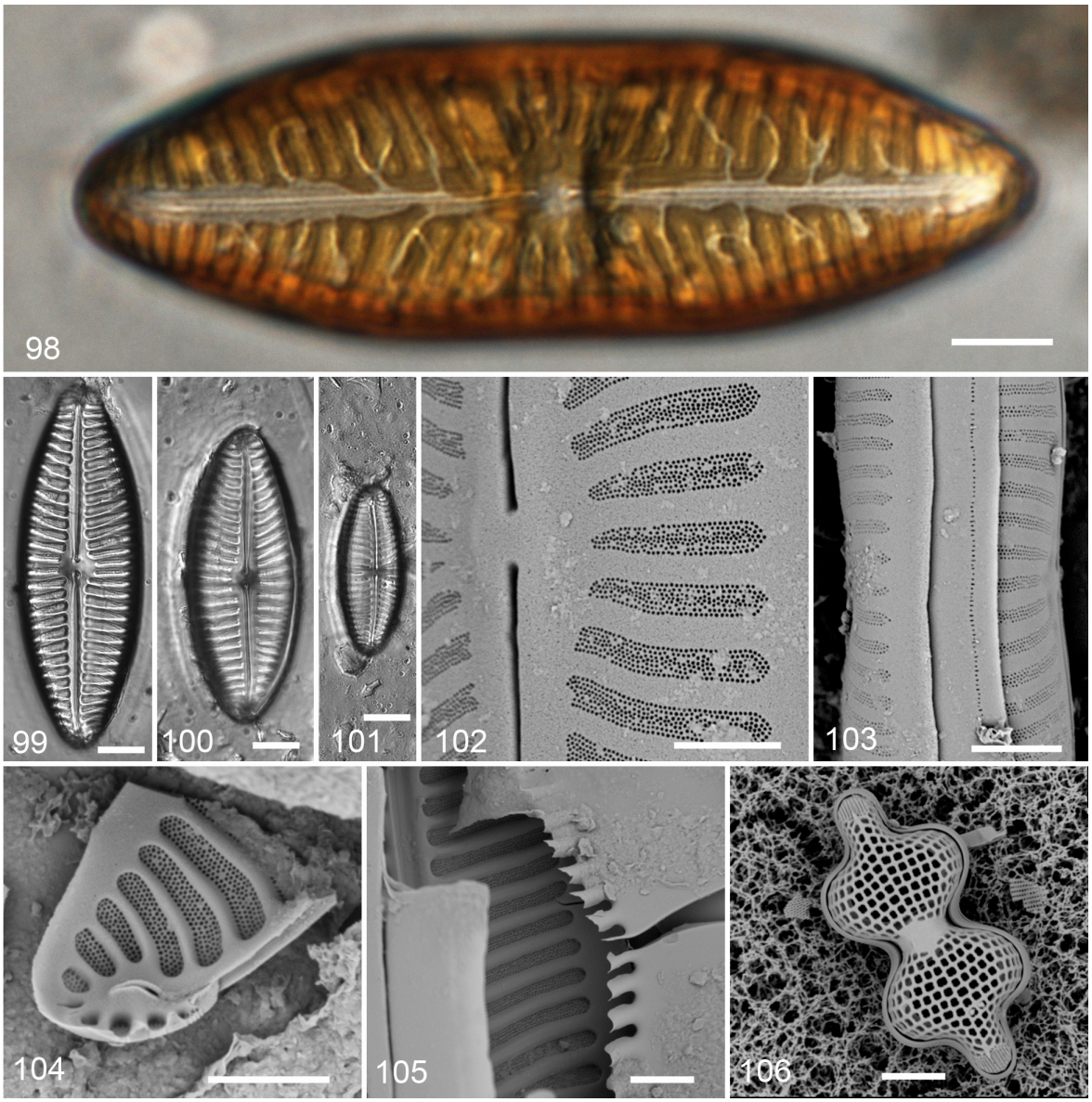
98
99
100
101
102
103
104
105
106

Figures 107–113. *Pogoneis bahrainii*. (GU44I-4) (SEM, except Fig. 107 DIC). Fig 107. Frustules in valve and girdle views. Fig. 108. Frustule in girdle view. Fig 109. SV, external view. Fig. 110. Detail of central area of RV. Fig. 111. Detail of apex of RV, showing the thickened "prow." Fig. 112. RV, internal view showing silica plate bordering the raphe and extending into interstrial costae. Fig 113. RV, detail of internal view showing apex. Scale bars: 107 = 10 µm; 108–113 = 1 µm.

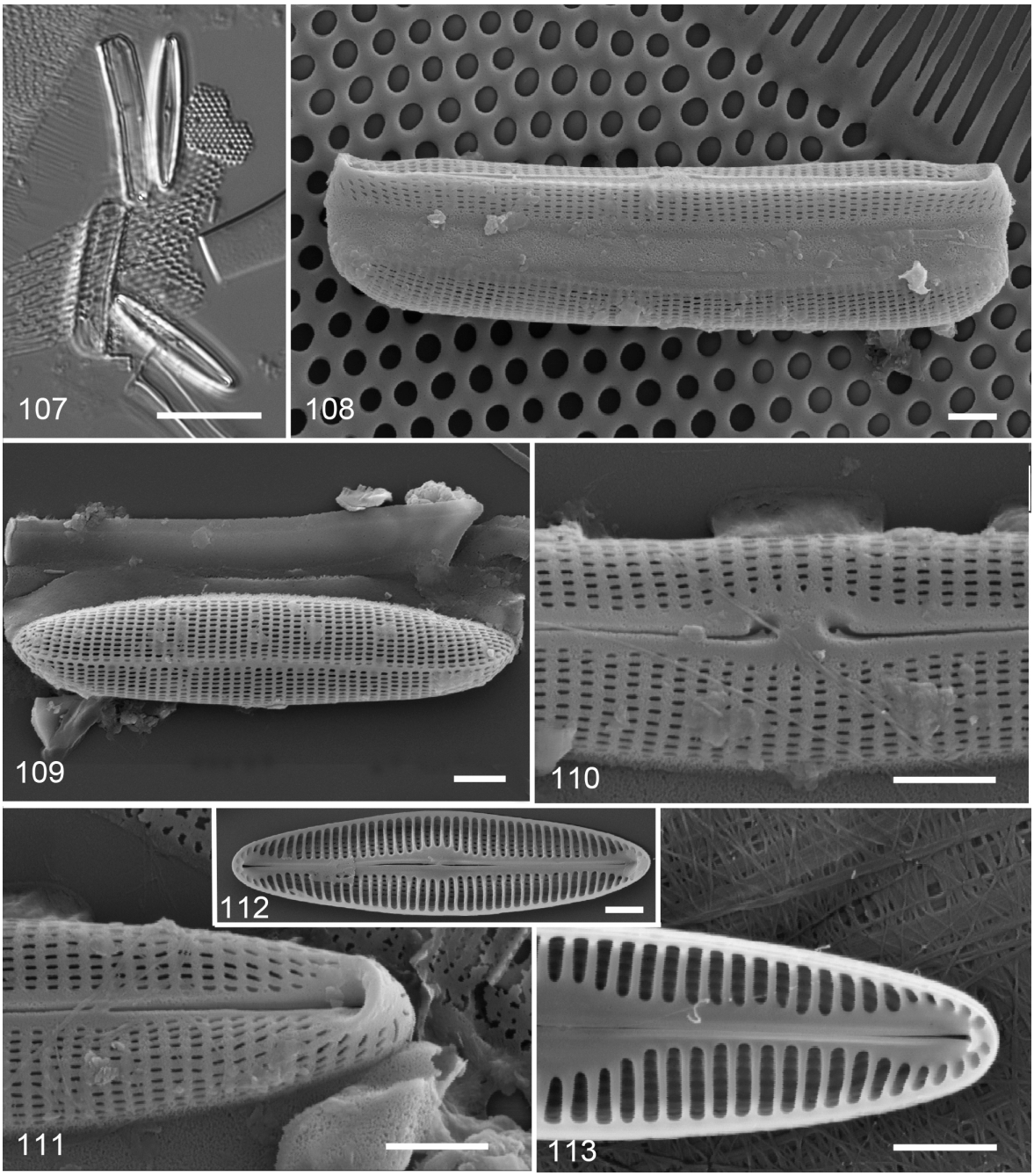
107
108
109
110
112
111
113

Figures 114–126. Figs 114–117. *Protokeelia cholnokyi*. Fig. 114. Valve in LM (GU44I-1) (DIC). Fig. 115. External view of valve (GU44J-2 / ECT3569), SEM; image courtesy of Elizabeth Ruck. Fig. 116. Internal view of valve (GU44Z-15) (SEM). Fig. 117. External, dorsal view of whole frustule showing girdle bands and dorsal faces of valves (SEM); courtesy of Elizabeth Ruck. Figs 118–126. *Psammodictyon pustulatum*. Figs 118, 119. Frustule at two focal planes (GU66F-7A) (DIC). Fig. 120. Valve from GU66A-3 (DIC). Fig. 121. Specimen from Nagasaki on Meister's slide 3509092. Fig. 122. Valve from Hustedt collection, slide W1/18, specimen from Vera Cruz, Mexico, image courtesy of Friedel Hinz. Fig. 123. External view of valve face (GU52Q-10a) (SEM). Fig. 124. Internal view of valve and part of the valvocopula. Arrows indicate where the valvocopula is broken. Inset shows full-resolution detail of valve margin and valvocopula, with the row of pores on the latter. Fig. 125. Frustule in oblique view showing the valves and girdle components. The ventral part of the valvocopula (vc) of the epivalve (ev) is visible at the front, and at the back the distal part of the valvocopula for the hypovalve (hv). Arrow indicates row of pores on the first pleura (p). Fig. 126. External detail of valve, showing the loculate character; arrow indicates row of pores on valvocopula. Scale bars: Figs 114–117, 123, 124 = 5 µm, Figs 118–122 = 10 µm, Figs 125, 126 = 2 µm.

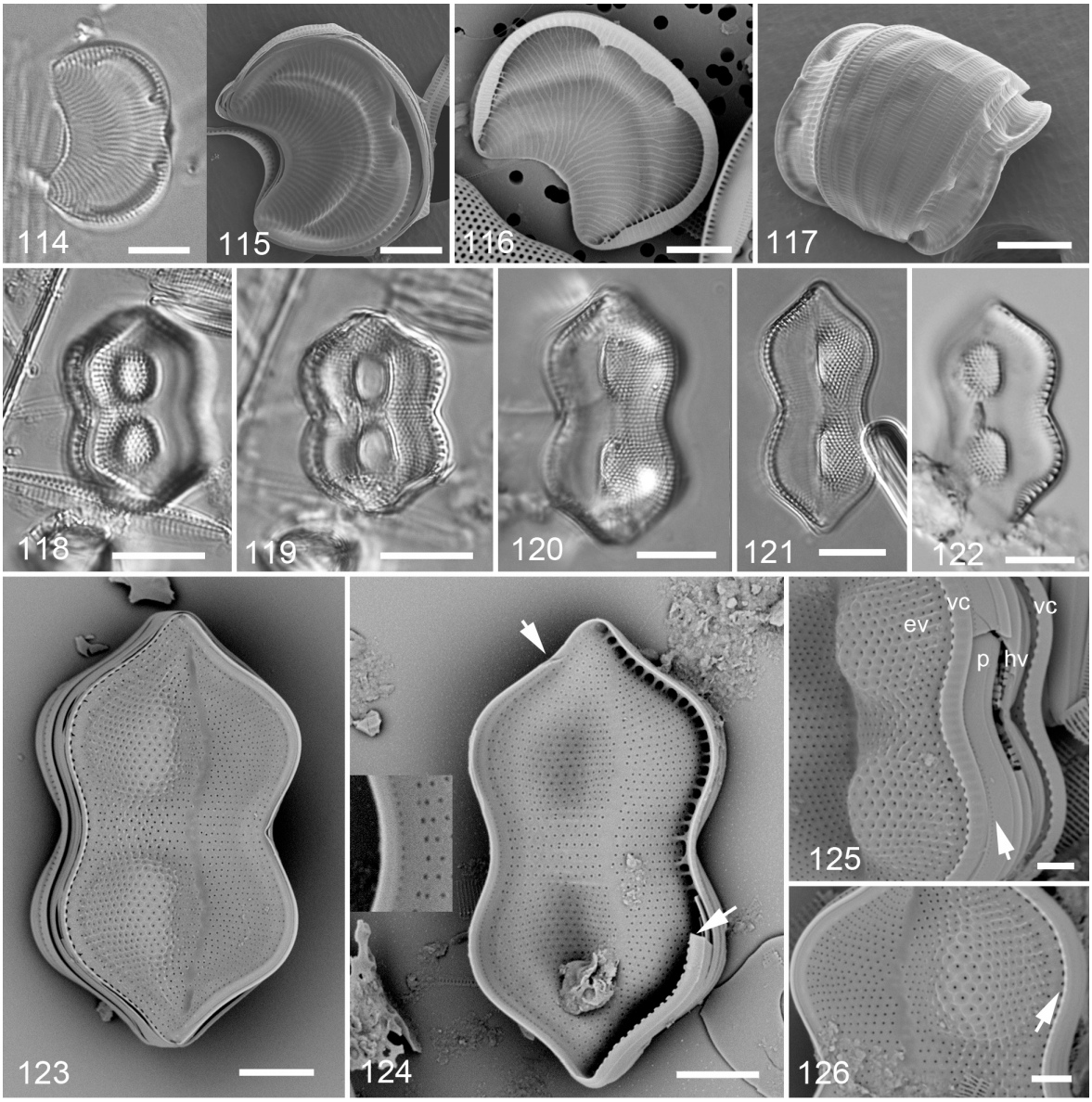
114
115
116
117
118
119
120
121
122
123
124
125
vc
vc
ev
p
hv
126

Figures 127–138. Figs 125–126. *Psammodictyon pustulatum* (GU66A-3) (SEM). Fig. 127. Oblique view of frustule showing linear pores on the dorsal valve face (arrow). In both Figs 127 and 128 the transition from the ventral to dorsal parts of the valvocopula is visible (arrowheads). Fig. 128. Apical view of frustule showing the distinctive topography of the ventral side of the raphe-keel, along with the linear pores on the dorsal side of the other valve (arrow) (two stacked images). Figs 129, 130. *Pteroncola inane* (SEM). Fig. 129. Frustule in girdle view (GU41D-1A). Fig. 130. Broken frustule showing internal and external valve faces, with the single row of internal pores (arrows) (Jordan collection, image by Misaki Ishizawa) (SEM). Figs. 131–138. *Rhoiconeis pagoensis.* Figs 131, 132. Same live cell in valve and girdle view showing plastids (GU7X-8) (DIC). Figs 133, 134. Holotype (valve view) and a girdle view from the same slide (GU7X-7) (DIC). Fig. 135. Frustule in valve view (GU7X-7) (SEM). Fig. 136. Frustule in girdle view; note the very short striae at the central area on the concave valve (GU7X-2) (SEM). Fig. 137. Detail of a pair of frustules showing difference in striae lengths at central area on convex and concave valves (GU7X-2) (SEM). Fig. 138. Apex of a frustule in girdle view showing the segmented valvocopula (S_1 and S_2) and two pleural bands (P_1 and P_2) (GU7X-5) (SEM). Scale bars: Fig. 136 = 10 µm, Figs 127–128, 131–135 = 5 µm, Figs 129, 130, 137, 138 = 2 µm.

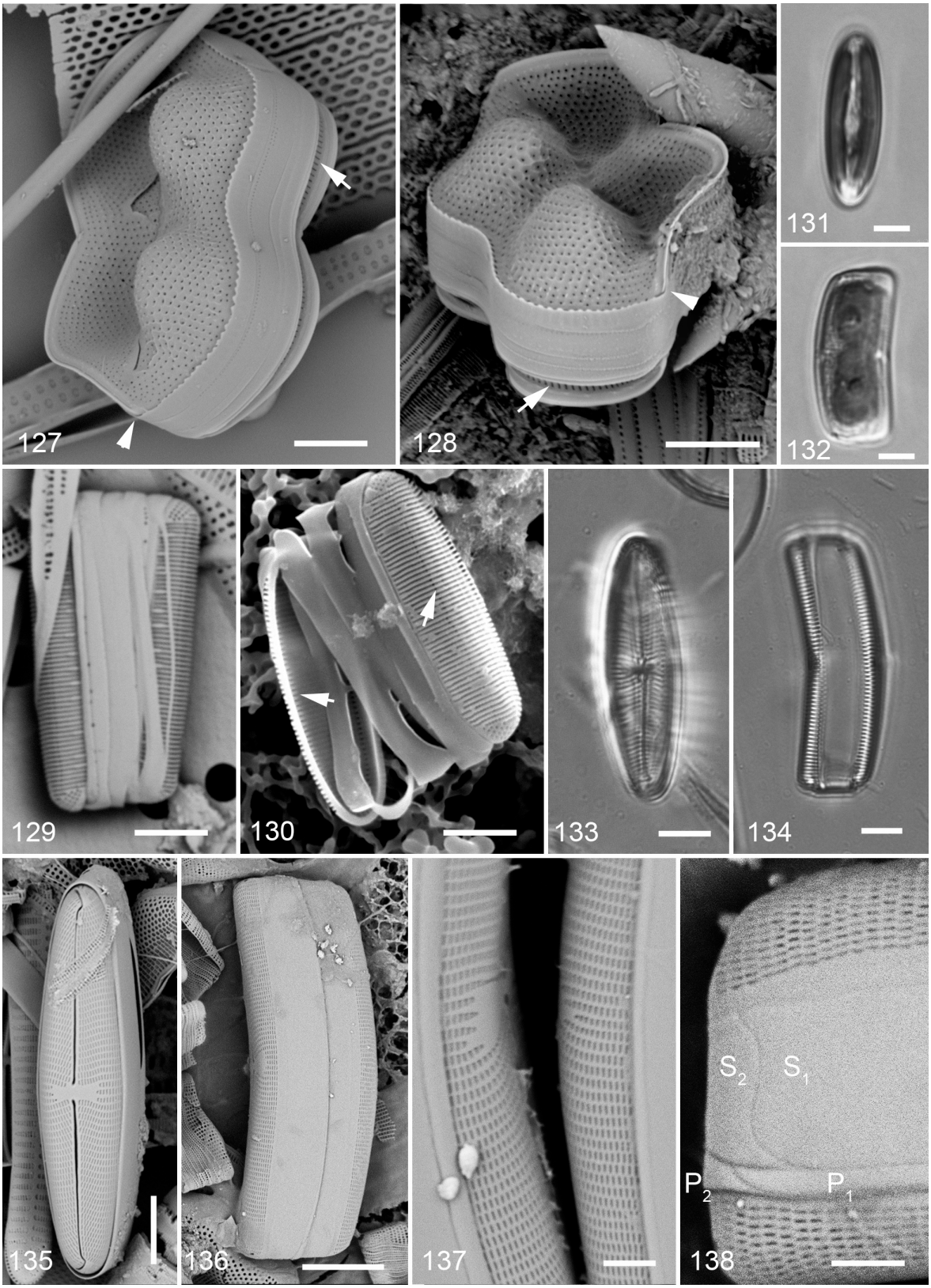
127
128
131
132
129
130
133
134
135
136
137
138
S2
S1
P2
P1

Figures 139–149. Figs 139–143. *Rhoicosigma compactum* (GU52N-7). Fig. 139. Three views of a live cell in different orientations (DIC). Figs 140, 141. Acid-cleaned valves showing the two contrasting raphe paths: convex valve nearly straight raphe, concave valve highly sigmoid (DIC). Fig. 142. External detail, convex valve, showing overlapping central raphe endings and pattern of striae (SEM). Fig. 143. Internal surface of concave valve. Figs 144, 145. *Seminavis robusta*, DIC (GU52Q-1a) and SEM (GU52Q-10a). Figs 146–149. *Surirella* cf. *fastuosa*. Fig. 146. Live cell show lobed plastid (GU66C-7). Fig. 147. Valve in DIC (GU44AQ-3) (two stacked images). Figs 148, 149. External and internal views of valve (GU66A-1, GU66A-2) (SEM). Scale bars: Figs 139–141, 143–149 = 10 µm, Figs 142 = 5 µm.

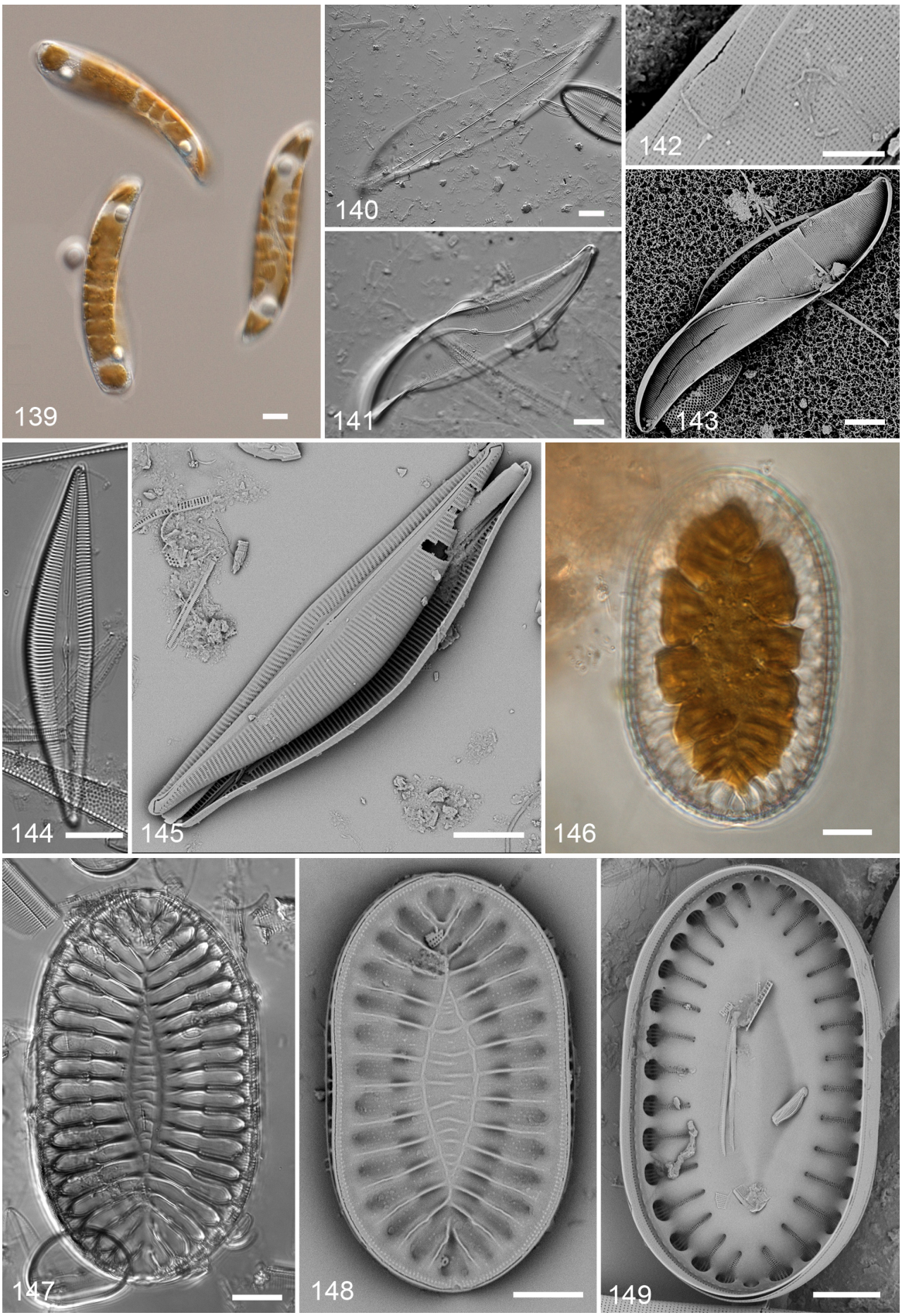
139
140
141
142
143
144
145
146
147
148
149